Upper ocean variability off NE Greenland (79°N) since the last glacial maximum reconstructed from stable isotopes in planktic foraminifer morphotypes

Robert F. Spielhagen[a] and Andreas Mackensen[b]

[a]GEOMAR Helmholtz Centre for Ocean Research, Wischhofstr. 1-3, D-24148 Kiel, Germany, Email: rspielhagen@geomar.de (*corresponding author*)

[b]Alfred Wegener Institute, Helmholtz Centre for Polar and Marine Research, Am Alten Hafen 26, D-27568 Bremerhaven, Germany

Abstract

We report on stable oxygen and carbon isotope data obtained on two different morphotypes of polar planktic foraminifers, i.e., fully encrusted and minor encrusted *Neogloboquadrina pachyderma*, from a sediment core taken on the NE Greenland continental margin. These morphotypes are supposed to live at different water depths of the upper water column in the area which today is strongly stratified, with a low-saline, cold-water layer at the surface. The paired isotopic data sets inform on temporal variations of past water salinity and temperature in the preferred water depth ranges of the investigated morphotypes and allow conclusions on the stratification of the upper water column. The radiocarbon-dated sediment core covers the time interval from 21 to 4 cal-ka, but the early part of the deglacial interval (18.6-12.7 cal-ka) is not represented, probably due to intense erosion by bottom currents. In sediments from the late last glacial maximum, oxygen isotope differences between thin-shelled and thick-shelled *N. pachyderma* are low and point at a weaker stratification with less freshwater than today near the surface. The carbon isotopes indicate a dense, perennial sea ice cover, very limited bioproduction, and the presence of a subsurface Atlantic Water layer. In the late deglaciation until ~10.3 cal-ka, the stable isotope values of both analyzed morphotypes are considerably lower, with significantly stronger amplitudes in the record of thin-shelled specimens than later on. The high-amplitude record stems from a laminated sediment sequence whose older part was deposited within just a few decades. The data are evidence of a strong freshwater event in the research area that probably started before 12.7 ka and may have reduced sea surface salinities by 4-5 practical salinity units. As freshwater sources we discuss both the disintegration of NE Greenland shelf ice and export from the Arctic Ocean interior. The event may have contributed to the weakening of the Atlantic meridional overturning circulation during the Younger Dryas cold event. For the early and mid-Holocene (10-4 cal-ka), the isotope data suggest a structure of the upper water column similar to today, with a well-developed halocline separating low-saline near-surface waters from the underlying Atlantic Water layer. A seasonally disintegrated sea ice cover allowed for a considerable planktic bioproduction.

Keywords: Quaternary, Paleoceanography, Arctic Ocean, Stable isotopes, Fram Strait, Greenland, Planktic foraminifers, Morphotypes, Salinity, Younger Dryas

1. Introduction

The western Fram Strait is the major conduit for the export of freshwater from the Arctic Ocean, both as sea ice and within the low-saline upper mixed layer (Dickson et al., 2007). The cold outflow plays an important role in the Atlantic meridional overturning circulation (AMOC) since it maintains the strong spatial temperature and salinity gradients in the area which are essential for deepwater renewal in the Greenland Sea (Aagaard et al., 1985). Excess freshwater export from the Arctic to the North Atlantic poses a threat to the AMOC (e.g., Manabe and Stouffer, 1995; Rahmstorf et al., 2015; Jackson and Wood, 2018) and may have triggered past instabilities of ocean circulation and climate (e.g., Condron and Winsor, 2012; Spielhagen and Bauch, 2015). To investigate examples of freshwater-driven instabilities in the geological past, the stable oxygen and carbon isotope compositions ($^{18}O/^{16}O$ and $^{13}C/^{12}C$, or $\delta^{18}O$ and $\delta^{13}C$) of planktic foraminifers (protozoa) from sediment cores provide useful tools. Their variations in the carbonate shells have been used to reconstruct spatial and temporal variations of near-surface salinity in high-latitude ocean waters (e.g., Sarnthein et al., 1995; Spielhagen et al., 2004, Keigwin et al., 2018). Most of these reconstructions were restricted to the water depth populated by morphologically left coiling planktic foraminifers *Neogloboquadrina pachyderma* (hereafter referred to as *N. pachyderma*). It is the only true polar species and found at various depths within the uppermost 500 m of the water column, depending on the location and the prevailing environmental conditions (Greco et al., 2019). Several morphotypes of *N. pachyderma* exist, from thin-walled to heavily encrusted specimens (cf. Eynaud et al., 2009; Eynaud, 2011) which were shown to have highly variable oxygen isotope compositions (e.g., Healy-Williams, 1992; Kohfeld et al., 1996; Hillaire-Marcel et al., 2004; El Bani Altuna et al., 2018). Most plankton tow data from regions with a quasi-perennial ice cover in the high latitudes suggest that the smaller, not or only minor encrusted specimens are usually younger and live in the very upper part of the habitat depth range, while the relative proportion of encrusted specimens increases with depth (Kohfeld et al., 1996; Simstich et al., 2003; Kozdon et al., 2009; Schiebel et al., 2017). A few contrasting observations from 78°N (Carstens et al., 1997) may be related to the advection of foraminifers from the east by the subsurface Return Atlantic Current (Fig. 1). Depending on the water mass structure and the related vertical variations of temperature and isotopic composition, $\delta^{18}O$ and $\delta^{13}C$ of *N. pachyderma* in the Arctic can be highly variable for different morphotypes and size fractions of this species (Healy-Williams, 1992; Hillaire-Marcel et al., 2004; Xiao et al., 2014; El Bani Altuna et al., 2018). Hillaire-Marcel et al. (2004) utilized the isotopic differences between size fractions of *N. pachyderma* in sediment cores from the Chukchi Sea (western Arctic Ocean) to reconstruct the water mass stratification. However, due to extremely low pre-Holocene sedimentation rates, their analysis was restricted to the last ~12,000 years (12 ka) with relatively uniform conditions. For the first time, in this paper we report on the $\delta^{18}O$ and $\delta^{13}C$ differences between relatively small specimens, which appear thin-walled, and larger, encrusted morphotypes of *N. pachyderma* in a sediment core from the NE Greenland continental margin (79.3°N) which recorded three environmentally distinctly different time intervals: The last glacial maximum, a major deglacial freshwater event, and the postglacial Holocene. The results reveal significant variations of the stratification and bioproduction in the upper water masses exported from the Arctic Ocean and hold important implications

for the interpretation of isotopic data sets from Arctic seas under variable climatic background conditions and for the deglaciation history of the NE Greenland shelf.

2. Environmental Setting

The continental slope off NE Greenland is a steep transition between the ~300 km wide NE Greenland shelf and the deep-sea area of the Fram Strait with water depths >3000 m (Fig. 1a). The shelf area south of the Kronprins Christian Land peninsula (81°N) is characterized by the C-shaped connected Westwind and Norske troughs (300-500 m deep) which reach the shelf break at c. 80.5 and 76.5°N. East of the troughs lie the shallower Belgica Bank (200-300 m) and the steep continental margin which plunges down to the Fram Strait.

The upper ocean circulation in the Fram Strait (Fig. 1a) is characterized by the northward flow of saline and relatively warm Atlantic Water (AW; T>3°C, S>35) in the West Spitsbergen Current (WSC) in the east and southward flowing, cold, low-saline waters of Arctic origin in the East Greenland Current (EGC; T<0°C, S<34.5) over the NE Greenland shelf and the adjacent continental margin (Aagaard and Coachman, 1968; Rudels et al., 2012; Håvik et al., 2017). A significant portion of the northward flowing AW recirculates to the west north of 78°N (Manley, 1995). At 79°N, 3-5°W the EGC is 100-150 m thick and separated by a strong halocline from recirculated AW beneath (Richter et al., 2018; Fig. 1). Water temperatures show a high intra-annual variability (-1.8 to +3°C) at 50-70 m depth, but the vast majority of daily measurements is between -1.5 and -1.8°C and higher temperatures, often occurring for for only few days, are scattered throughout all seasons (de Steur et al., 2014). The interannual variability of mean annual temperatures at this depth is low and within the range of -1.5 to -1.8°C (de Steur et al., 2014). In average winters (1978-2010; data from nsidc.org), the NE Greenland shelf and continental margin north of 76°N are covered by sea ice (Fig. 1a). The average summer sea ice margin runs northeastward across the Fram Strait from the Greenland continental margin at ~78°N to the Yermak Plateau margin at ~80.5°N. In exceptional summers of the last decade, large parts of the NE Greenland shelf south of 82°N were almost free of sea ice.

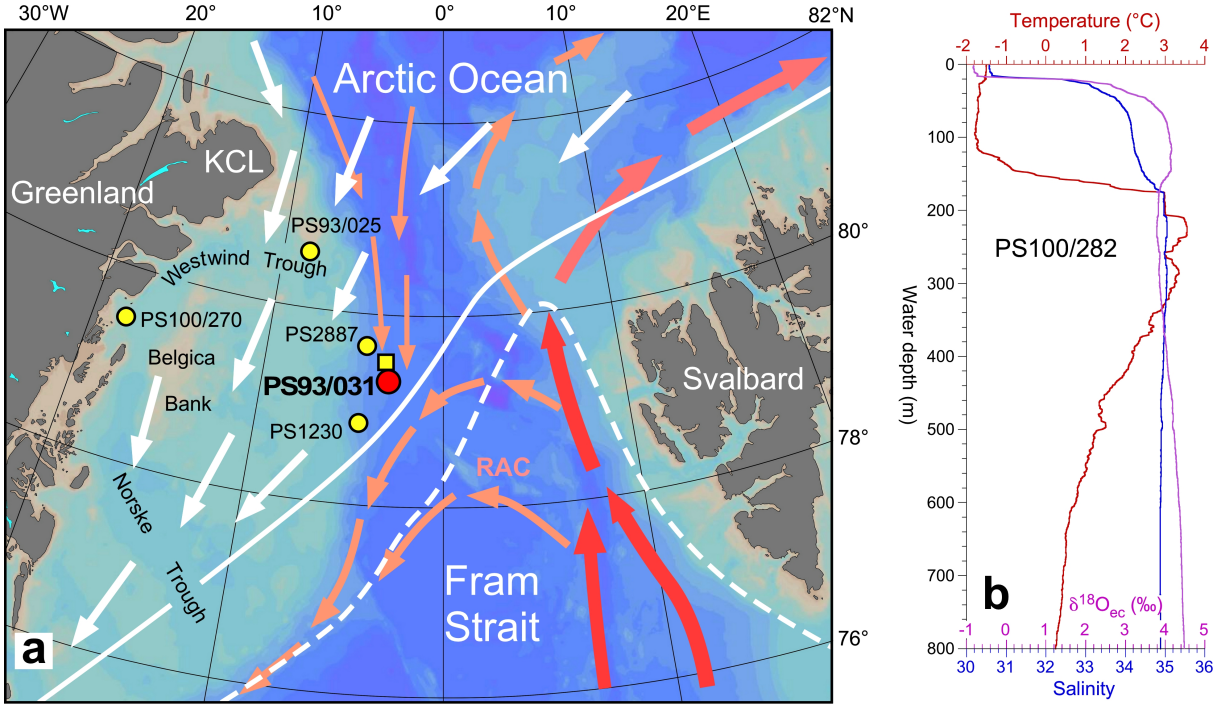

Fig. 1

a) Bathymetric map of the Fram Strait with deep-sea areas (water depth >400 m) shown by bluish colors. Locations of cores mentioned in the text are indicated by red and yellow circles. The yellow square marks the location of oceanographic station PS100/282. Red arrows display the circulation pattern of Atlantic Water, with lighter colors indicating subsurface flow (after Richter et al., 2018). Full and stippled white lines mark the average positions of summer and winter sea ice margins (1981-2010, from nsidc.org). White arrows show the average ice drift pattern. RAC = Return Atlantic Current. Bathymetric map created by Ocean Data View (Schlitzer, 2020).

b) Data of water temperature (red) and salinity (blue) in the upper 800 m at station PS100/282 (Kanzow et al., 2017) close to core site PS93/031. Calculated $\delta^{18}O$ values for equilibrium calcite ($\delta^{18}O_{ec}$) are shown in pink..

3. Materials and Methods

Box core PS93/031-5 was obtained from 2135 m water depth on the NE Greenland continental slope (79°20.97'N, 3°31.43'W) during expedition PS93.1 of RV Polarstern in July 2015 (Stein, 2016; Fig. 1a). It had an uneven surface with abundant agglutinated and calcareous foraminifers. The recovered 37.5 cm long sequence consists of brownish and grayish muds with common small (<2 cm) dropstones (ice-rafted detritus, IRD) in the lower part (Fig. 2). To avoid compression of the sediment sequence in the 50x50 cm metal box, it was opened at one side and a 50x12x8 cm plastic archive box was pressed horizontally into the sediment. Thin sediment slabs for X-ray photos were taken likewise. These photos (Fig. 2) reveal that

the brownish IRD-rich layer at the core base is overlain at ~25 cm core depth by a ~7 cm thick IRD-free, distinctly laminated sequence of brownish gray color. Above this layer we find ~4 cm of grayish brown sediments with only faint laminae visible in the X-ray photos. The uppermost 14 cm consist of strongly bioturbated dark brown mud with common IRD in its upper part.

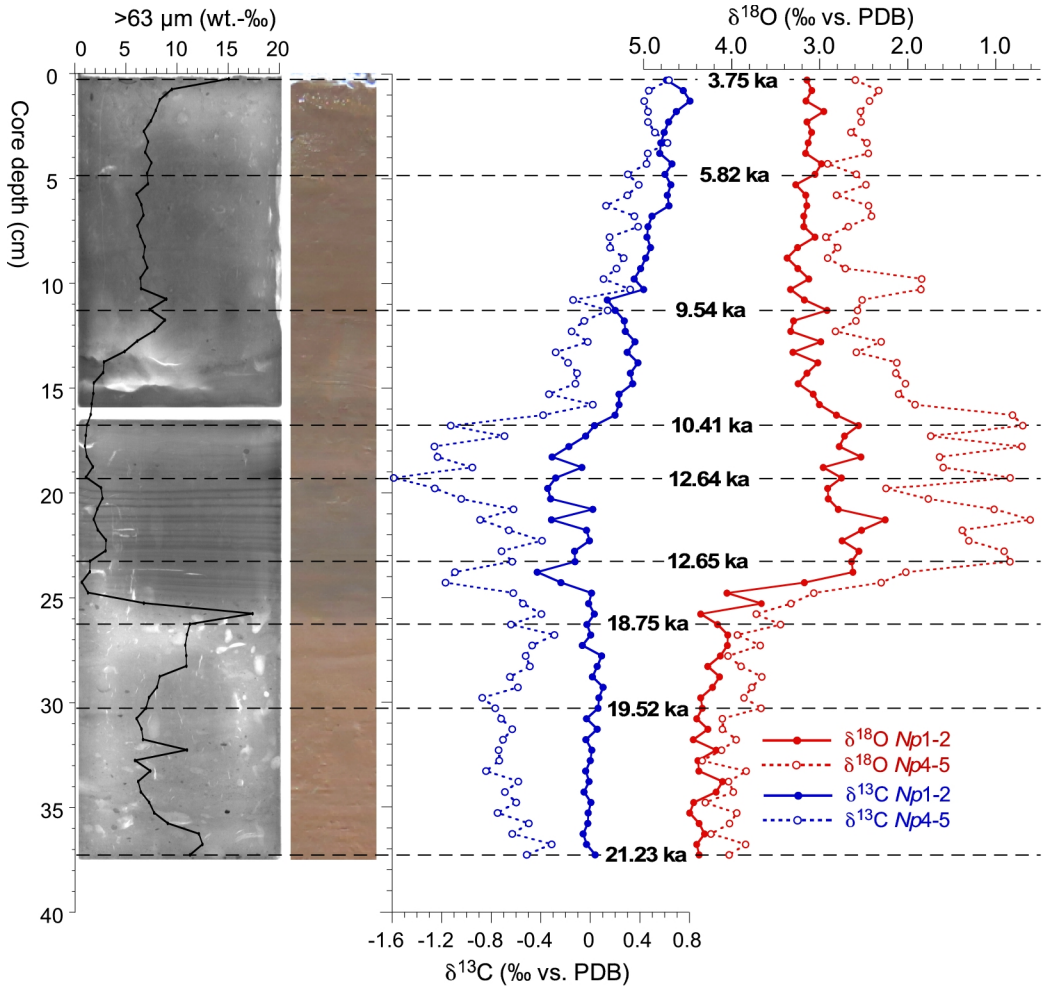

Fig. 2

Left: X-ray photos (from Stein, 2015), coarse fraction data, and photo of sediment sequence of box core PS93/031-5.

Right: Oxygen and carbon isotope data of *N. pachyderma* morphotypes 1-2 and 4-5 (*Np*1-2, *Np*4-5). Radiocarbon-dated horizons are marked by stippled horizontal lines, with calibrated ages given in kiloyears.

Core PS93/031-5 was sampled continuously in 0.5 cm intervals. Samples were freeze-dried, weighed, washed through a 63 µm mesh with deionized water, and dried at 50°C. The remaining coarse fraction was split into several size fractions. For isotopic analyses, two sets of planktic foraminifers *N. pachyderma* were picked from the 100-250 µm fraction of each sample. During foraminifer selection, we followed the morphotype concept of Eynaud et al.

(2009) and Eynaud (2011). One set comprised 25 relatively large, fully encrusted specimens visually resembling morphotypes 1 and 2 (hereafter referred to as *Np*1-2; Fig. 3), the other 40 relatively small specimens resembling morphotypes 4 and 5 (*Np*4-5; Fig. 3). From visual inspection under a binocular, the latter appear thin-walled, when compared to *Np*4-5, and often translucent. In many ways, *Np*4-5 and *Np*1-2 resemble the "adult" and "terminal" stages, respectively, of *N. pachyderma* development as identified by Berberich (1996). From visual inspection we estimate that the average diameter of *Np*4-5 was 50-70% of the diameter of *Np*1-2. By analyzing pooled samples, we assume to balance possible isotopic differences between single specimens which may result from intra-annual and interannual oceanographic variations. Oxygen and carbon isotope ratios ($\delta^{18}O$, $\delta^{13}C$) were measured in the stable isotope laboratory of the Alfred Wegener Institute in Bremerhaven with a Finnigan MAT 253 gas mass spectrometer coupled to the automatic carbonate preparation device Kiel IV. The mass spectrometer was calibrated via international standard NBS19 to the PDB scale. Results are given in δ-notation vs. VPDB. The precision of $\delta^{18}O$ and $\delta^{13}C$ measurements, based on an internal laboratory standard (Solnhofen limestone) measured over a 1-year period together with samples, was better than ±0.08 and ±0.06‰, respectively.

Oxygen isotope data of equilibrium calcite ($\delta^{18}O_{ec}$) in the water column were calculated using the paleotemperature equation of O'Neil et al. (1969)

$$T = 16.9 - 4.38\,(\delta^{18}O_{ec} - \delta^{18}O_w) + 0.1\,(\delta^{18}O_{ec} - \delta^{18}O_w)^2$$

and relations between water isotope ($\delta^{18}O_w$) and salinity (S) of $\delta^{18}O_w = 1.35\ S - 46.8$ for $S>32.7$ (derived from data of Rabe et al., 2009, and Pados et al., 2015) and $\delta_w = 0.04\ S - 3.89$ for $S<32.7$ (Rabe et al., 2009). $\delta^{18}O_w$ was converted to $\delta^{18}O$ of calcite (here: $\delta^{18}O_{ec}$) for the paleotemperature equation following Bemis et al. (1998): $\delta^{18}O_{ec} = 0.9998\ \delta^{18}O_w - 0.2‰$.

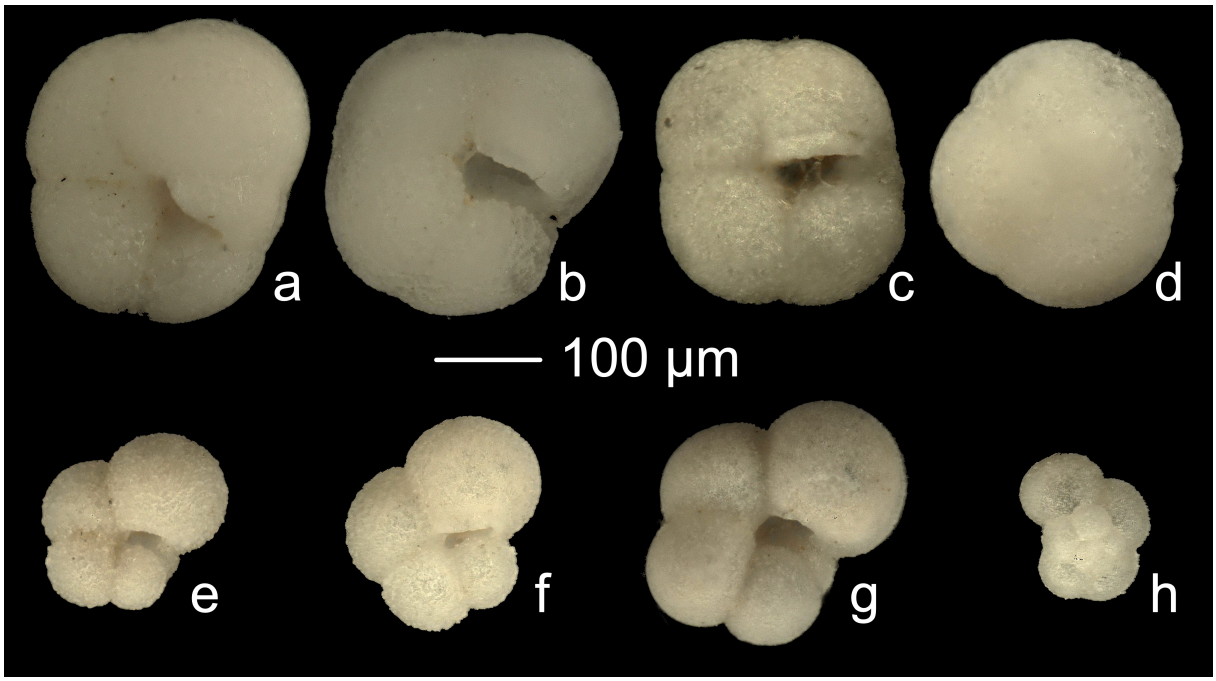

Fig. 3: Layered photographs of *N. pachyderma* morphotypes 1-2 (a-d) and 4 (e-h) from core PS93/031-5 (18.5-19.0 cm).

For age control on PS93/031-5, ~2000 specimens of *Np*1-2 per sample were picked from nine selected samples and dated at the AMS-^{14}C facility of the Leibniz Laboratory for Age Determination and Isotope Research of Kiel University. Results (Table 1) were converted to calibrated years by the CALIB 8.2 program (Stuiver et al., 2021). Since the MARINE20 data set is not suitable for samples from polar regions (Heaton et al., 2020), we used the IntCal20 data set for calibration and applied a reservoir correction (R) of 550 years. This R value was determined from recent (pre-bomb age) molluscs sampled in East Greenland (Tauber and Funder, 1975), has been used for calibration of other samples from this region (Nørgaard-Pedersen et al., 2008; van Nieuwenhove et al., 2020), and lies in the range of values determined from western Svalbard (~438-450 yr; Mangerud et al., 2006) and fjords entering the open Arctic Ocean in the Canadian Arctic Archipelago (~700-800 yr; Mangerud et al., 2006; Coulthard et al., 2010). We note that assuming a higher or lower reservoir correction will not significantly alter the major conclusions of this paper. The temporal resolution of sampling is sufficient to allow unambiguous statements on the isotopic differences between *Np*1-2 and *Np*4-5 for the three time intervals discussed. To plot isotope data versus age, we determined sediment ages with the Bayesian R package *Bacon* (Blauuw & Christen, 2011), the IntCal20 data set, and a reservoir correction of 550 years. Within *Bacon*, we accounted for a hiatus at 25 cm and an age difference of 20 years (from counting the laminae) between 19 and 25 cm. In the following, ages are given as calibrated kiloyears (ka).

Table 1

Results of radiocarbon datings from core PS93/031-5 performed on planktic foraminifers *N. pachyderma* (morphotype 1-2). Calibrated ages were determined with the Calib 8.2 program, the IntCal20 data set and a reservoir correction of 550 years (see section 3 for details)

Interval (cm)	Sample code	14C age (yr)	Calibrated age mean (yr)	Cal. age (yr) 2σ range
0.0-0.5	KIA-53302	4023 ± 28	3752	3687-3832
5.0-5.5	KIA-53303	5630 ± 35	5815	5741-5911
11.0-11.5	KIA-53304	9130 ± 40	9540	9482-9564
16.5-17.0	KIA-53766	9790 ± 40	10405	10254-10511
19.0-19.5	KIA-53767	11140 ± 45	12635	12592-12714
23.0-23.5	KIA-53768	11165 ± 45	12652	12608-12723
26.0-26.5	KIA-53305	15970 ± 65	18748	18634-18864
30.0-30.5	KIA-53769	16730 ± 65	19523	19334-19648
37.0-37.5	KIA-53770	18135 ± 70	21227	20966-21440

4. Results

4.1 Chronology and coarse fraction content

The age range of the core covers the period between 21.2 ka for the lowermost sample (37.0-37.5 cm) and 3.8 ka for the core-top (Table 1). The three datings from the lowermost, IRD-rich unit (25.0-37.5 cm, 6-12% coarse fraction) reveal a sedimentation rate of ~4 cm/ka for the period 21.2-18.6 ka which corresponds to the younger part of the last glacial maximum (LGM). The abrupt change in coarse fraction content with a peak value at the top (19%), the high amount of coarse IRD visible in the X-ray photos (Fig. 2), and the uneven upper boundary of this unit, which is overlain by a laminated sequence, suggest the presence of a lag deposit and a hiatus in PS93/031-5 which covers the interval of 18.6-12.7 ka. Age determinations between dated layers are based on linear inter-/extrapolation and consider the hiatus at 25 cm.

Three dates are available from the fine-grained laminated units, of which the two older ones are equal (12.64 and 12.65 ka) within their uncertainty ranges. The perfect lamination precludes any influence of bioturbational sediment mixing. We suppose that the lower, gray laminated unit was deposited very rapidly and that the individual laminae may represent annual layers. As indicated by the age of 10.4 ka at 16.5-17.0 cm, the faintly laminated sequence at 14-18 cm was deposited more slowly (~2 cm/ka).

The available datings and the relatively invariable coarse-fraction content (6-9 weight-%) suggest rather uniform sedimentation with rates of ~2 cm/ky for the uppermost dark brownish unit which was deposited from ~9.9±0.2 to 3.8 ka and thus largely represents the Early and mid-Holocene. Most likely, Late Holocene sediments are missing due to strong bottom currents, as indicated by the high abundances of agglutinated foraminifers (cf. Kaminski et al., 2015) and coarse fraction in the core-top sample (Fig. 2), which may be a relict sediment.

4.2 *Neogloboquadrina pachyderma* isotope data

In samples from the late LGM (25.5-37.5 cm), $\delta^{18}O$ values of *Np*1-2 and *Np*4-5 are 4.6-4.2‰ and 4.4-3.7‰, respectively, with an average difference (mean) of 0.36‰ (Figs. 2, 4). Standard deviations of mean values are <0.1‰, unless otherwise stated. In some of these samples the apparent differences are within the error range of the measurements. The $\delta^{13}C$ data of *Np*1-2 are almost constant in this interval (0.01‰) while those of *Np*4-5 are 0.3-0.9‰ lower (average difference 0.61‰). At the boundary to the overlying unit the differences are increasing. Very likely this is a result of the sampling procedure which could not ensure a precise differential sampling of the two units due to the uneven boundary. Values from the transition zone (23.5-25.5 cm) were therefore not included in the calculations.

In the laminated units (16.0-23.5 cm) $\delta^{18}O$ values of both analyzed morphotypes are significantly lower than further below (Figs. 2, 4). With one exception, $\delta^{18}O$ of *Np*1-2 ranges within 2.5-3.0‰ while values of *Np*4-5 show a higher variability (0.6-1.8‰). The average difference between morphotypes is 1.56±0.12‰ but in several samples it is >2‰. The $\delta^{13}C$ values of *Np*1-2 show a somewhat higher variability than in the late LGM. Some are on the same level (~0‰) but five samples are around -0.3‰. Like for $\delta^{18}O$, *Np*4-5 show significantly higher

amplitudes for $\delta^{13}C$ (range: -0.6 to -1.6‰), with an average difference of 0.77‰ to the $\delta^{13}C$ values of *Np*1-2.

Omitting a transitional sample from 15.5-16.0 cm, $\delta^{18}O$ values of *Np*4-5 and *Np*1-2 from the Early and mid-Holocene interval (0-15.5 cm) are between those from the LGM and the laminated unit (Figs. 2, 4). Again, *Np*1-2 shows a narrower range (3.0-3.4‰) than *Np*4-5 (2.0-3.0‰, except two samples at ~10 cm), with an average difference of 0.69‰. The $\delta^{13}C$ ranges of *Np*1-2 (0.1-0.8‰) and *Np*4-5 (-0.3 to 0.8‰) are relatively large, but the average difference is small (0.27‰), compared to the other two time intervals.

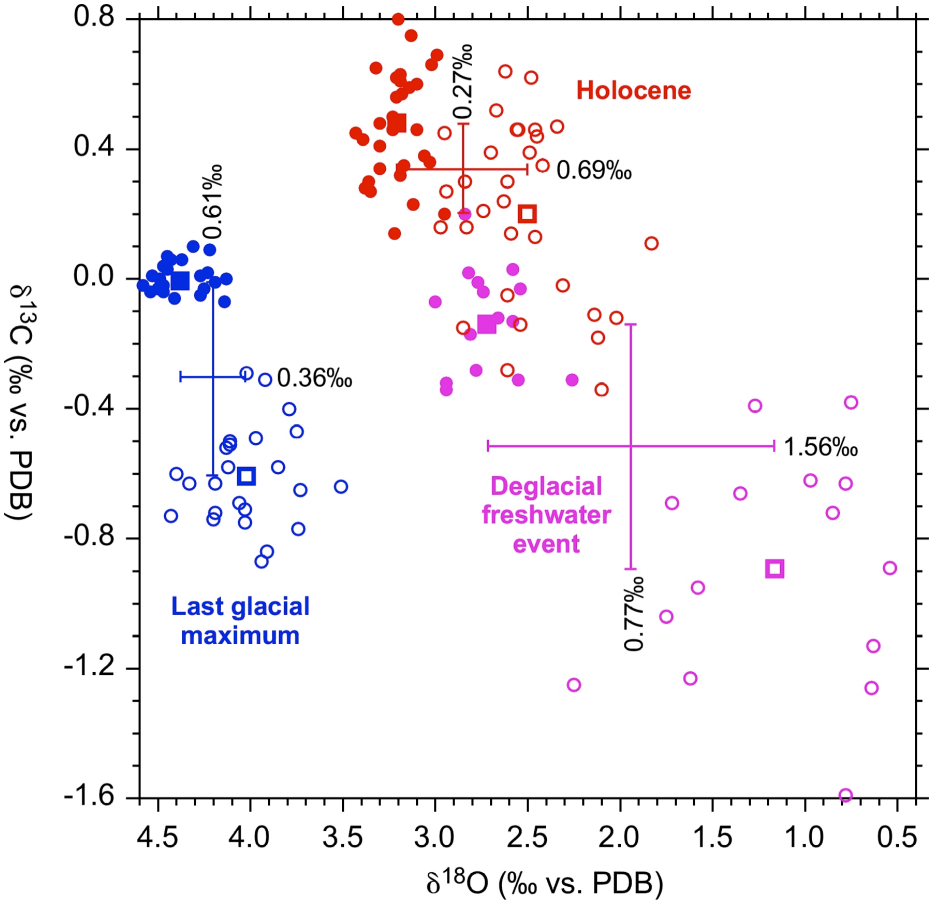

Fig. 4

Plot of carbon vs. oxygen isotope data, grouped for late LGM data (blue), the deglacial freshwater interval data (pink), and Holocene data (red). The crosses indicate the differences between mean data (squares) for morphotypes *Np*1-2 (full symbols) and *Np*4-5 (open symbols).

5. Discussion

5.1. Stable isotopes in planktic foraminifers as environmental recorders

In general, the variability in the isotopic composition of planktic foraminifers reflects corresponding changes of temperatures and/or the isotopic composition of sea water and its dissolved inorganic carbon (DIC) in which the individuals calcify their tests (Epstein et al.,

1953; Erez and Luz, 1982). For oxygen, the isotopic composition of sea water may vary due to the preferential storage of ^{16}O in continental ice during glaciations ("ice volume effect") and the return of ^{16}O-enriched freshwater from continents to the ocean, be it as meltwater or riverine input. In Fram Strait waters with salinities >33.5, as prevailing below ~30 m along the NE Greenland continental margin (Håvik et al., 2017; Richter et al., 2018), there is a quasi-linear relationship between salinity and $\delta^{18}O_w$ (Rabe et al., 2009), as seen also in the interior Arctic Ocean (Bauch et al., 1995). In the area of site PS93/031 >80% of all *N. pachyderma* live in the upper 100 m of the water column (Pados and Spielhagen, 2014) where temperatures are (despite some outliers) almost constant and close to the freezing point (-1.7°C; Fig. 1). *A priori* it cannot be excluded that seasonal variations of temperature and $\delta^{18}O_w$ (related to salinity) may be responsible for the isotopic differences observed between the morphotypes in our samples, in particular if the relative abundances of the morphotypes were variable through the seasons. To test the potential influence of such a seasonal effect, we compared $\delta^{18}O_{ec}$ values calculated from monthly temperature and salinity data (April-October, if available) from six sectors on the NE Greenland continental margin obtained from the World Ocean Atlas 2018 (WOA 2018) (Boyer et al., 2018; Locarini et al., 2018; Zweng et al., 2018; Fig. 5). In all sectors (except 79°N 5.5°W), $\delta^{18}O_{ec}$ values from ~40 m are lower than at ~80 m. Differences are higher in the North and in the West and amount to 0.3-1.5‰. Differences on the longitude of PS93/031 (3.5°W) are 0.2-0.8‰ and thus in the range of differences between *Np*1-2 and *Np*4-5 in Holocene samples. The data from July and September (JS) always plot very close to each other. Values from August (i.e., the middle of summer off NE Greenland) are variable in the data sets. At 40-100 m depth they are very close to JS values at 2.5°W, lower than JS values at 3.5°W, and higher than JS values at 5.5°W. Overall, it seems difficult to find systematic differences of $\delta^{18}O_{ec}$ values between the individual months of the summer season in our research area.

Little is known about the seasonal abundance distribution of *N. pachyderma* morphotypes or size fractions in the Arctic. Jensen (1998) found that at 72°N 7.7°W (in ice-covered waters of the Greenland Sea) the small specimens (which may to a large part be *Np*4-5) have their abundance maximum very late in the summer season (October). Similar observations were made southeast of Greenland (Jonkers et al., 2013). According to the monthly vertical $\delta^{18}O_{ec}$ profiles from the 79°N3.5°W sector (Fig. 5), late summer specimens (assumed to be mostly Np4-5) from September should show higher $\delta^{18}O$ values than larger (encrusted) specimens from earlier in the year (August) if both calcified in the same water depths. However, this is opposite to what we find in our Holocene samples. We conclude that the seasonal abundance distribution of *N. pachyderma* morphotypes (and size fractions) apparently does not exert a strong influence on the distribution of $\delta^{18}O$ values found and that it is rather the vertical variability of $\delta^{18}O_{ec}$ which is reflected in the *N. pachyderma* in the samples from site PS93/031. Considering the weak intra-summer temperature changes (T = -1.5°C ±0.5°C between 0 and 100 m, data from WOA 2018).we expect an almost negligible influence of vertical or seasonal temperature changes on the $\delta^{18}O$ of foraminifers in individual samples. Accordingly, we will mostly interpret the $\delta^{18}O$ variability in our foraminiferal records in terms of salinity changes. If applicable, the ice volume effect and potential temperature changes are also considered.

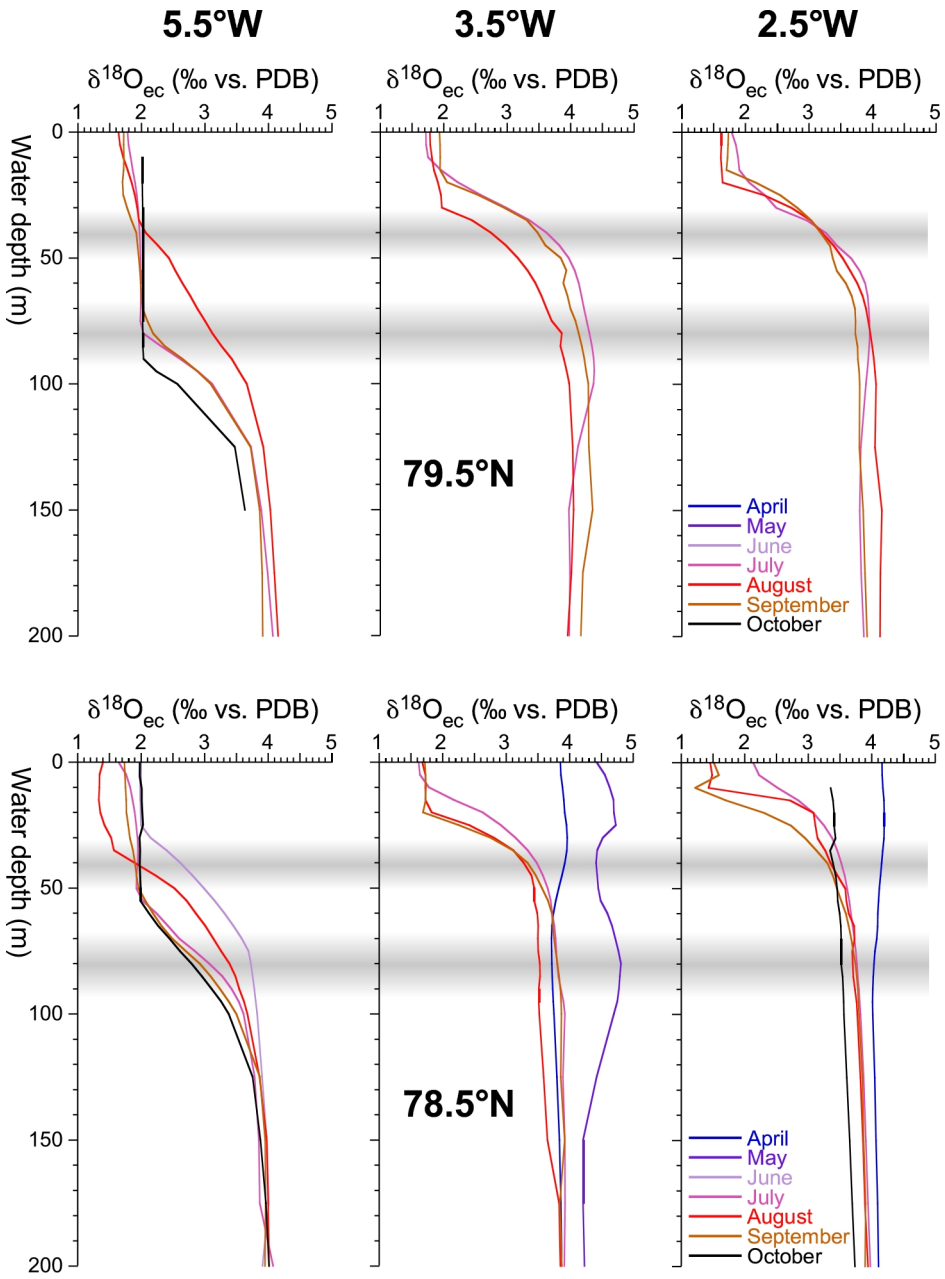

Fig. 5

Oxygen isotope data of equilibrium calcite calculated for the upper 200 m of the water column in six 1° x 1° sectors on the NE Greenland continental margin. Coordinates of the sector centers are given on the top margin and in the center row. Data were calculated using temperature and salinity data (averaged decades) from the World Ocean Atlas (Boyer et al., 2018; Locarini et al., 2018; Zweng et al., 2018). Grayish horizontal bars mark water depths assumed to represent average habitat depths of *Np*4-5 (~40 m) and *Np*1-2 (~80 m).

Exact calcification depths for the investigated morphotypes cannot be determined from our data. According to plankton tow data, in perennially ice-covered Arctic seas the encrusted specimens of *N. pachyderma* were found deeper in the water column than the non-encrusted ones (Kohfeld et al., 1996; Simstich et al., 2003; Schiebel et al., 2017). Eynaud (2011, p. 5) notes that "the wall texture and the degree of encrustation is also a discriminating feature of

the different morphotypes". Combining both observations, in this study we suppose that the isotopic composition of *Np*4-5 mostly reflects conditions in a shallower layer than the one of *Np*1-2 which likely integrates over shallow and somewhat deeper waters. Supporting evidence comes from the fact that in none of our samples both the carbon and the oxygen isotope compositions of *Np*1-2 and *Np*4-5 were similar, which would be expected if they had the same habitat. The overall positive differences in $\delta^{18}O$ between *Np*4-5 and *Np*1-2 (average 0.69‰ in the Holocene) are very much similar to the difference in $\delta^{18}O$ of equilibrium calcite calculated for waters from 40 and >65 m (Fig. 1b). Again, this observation is in line with the assumption that *Np*1-2 specimens have formed their shells in a depth range reaching deeper than that of *Np*4-5. According to the above considerations, from the observed isotopic differences between both types we will draw semiquantitative estimates on the vertical variation of water mass parameters (mostly salinity) and the stratification in the investigated time intervals. Over time these variations, in addition to changing ice coverage and food availability, may have induced shifts in the habitat depths of the foraminifers (see Greco et al., 2019, for modern relations).

Size-dependent isotopic differences among *N. pachyderma* specimens have been observed by several sediment and plankton tow studies (e.g., Healy-Williams, 1992; Kohfeld et al., 1996; Hillaire-Marcel et al., 2004; Jonkers et al., 2013; Xiao et al., 2014; El Bani Altuna et al., 2018) and attributed to a variety of effects (e.g., temperature variability, seasonality, ontogenetic/metabolic effects). We did not perform our measurements on specimens selected strictly size-dependent. Still, a size-dependent isotopic variability is likely inherent to the observed isotopic differences between *Np*1-2 and *Np*4-5 and probably related to the supposed encrustation on *Np*1-2 at greater depths. An important finding of our study, however, is that the differences of both $\delta^{18}O$ and $\delta^{13}C$ between the morphotypes are strongly diverse when three environmentally different time intervals are compared. These differences can thus not be ascribed to a constant size effect and will be discussed in more detail further below. Variable vital effects (offsets between the isotopic value of foraminifers and the calculated value of equilibrium calcite) of *N. pachyderma* have been ascribed to changes in temperature and water masses (e.g., Bauch et al., 1997; Simstich et al., 2003; Nyland et al., 2006). As will be discussed below, we do not find evidence for strong temperature variability or changes in the general structure of the water column off NE Greenland in the time intervals considered. Accordingly, we do not presume a strong influence of vital effects on the isotopic differences between the morphotypes.

On the timescales discussed here, the carbon isotope ratio in DIC depends on the atmosphere-ocean exchange of CO_2 and the bioproduction and decomposition of carbon in the water column. The LGM-Holocene difference of $\delta^{13}C$ in atmospheric CO_2 was only ~0.1‰ (Schmitt et al., 2012) and can thus be neglected here. High primary production results in high $\delta^{13}C$ values of the DIC because ^{12}C is preferentially taken for photosynthesis (Kroopnick, 1974; Fogel and Cifuentes, 1993), leaving the upper waters enriched in ^{13}C. By microbial degradation of organic matter in the less well ventilated layers below the productive zone of the water column, ^{12}C is returned and $\delta^{13}C$ values are usually significantly lower. This general pattern is found also in modern waters in the research area (Bauch et al., 2015; Pados et al., 2015) which are strongly stratified due to vertical temperature and salinity differences (Fig. 1b). Accordingly,

we will interpret the $\delta^{13}C$ values of the analyzed planktic foraminifers in terms of bioproduction and decomposition of carbon from organic matter, indicating variable degrees of ventilation and stratification. However, terrestrial sources of carbon with specific isotopic signatures will also be considered. We note that variations in the carbonate ion concentration in seawater can have a strong effect on the offset between the $\delta^{13}C$ values of DIC and foraminifers (Spero et al., 1997). Since we do not have information on such variations in our research area in the past, some caution must be applied with interpretations of our $\delta^{13}C$ records, in particular when they are not backed up by other data.

5.2. The (late) last glacial maximum

The LGM $\delta^{18}O$ values of ~4.4‰ in *Np*1-2 from PS93/031-5 are typical for thick-shelled *N. pachyderma* in deep-sea LGM samples from the Nordic Seas and the Fram Strait (cf. Sarnthein et al., 1995; Nørgaard-Pedersen et al., 2003). Moreover, the Holocene average (3.2‰) resembles the values of sediment surface samples from the western Fram Strait (cf. Bauch et al., 2001; Pados et al., 2015). The resulting $\delta^{18}O$ change from the LGM to the Holocene in *Np*1-2 is thus equivalent to the global ocean glacial-interglacial shift originating from the preferential storage of ^{16}O in continental ice sheets which is 1.1-1.4‰ (Mix et al., 2001). We conclude that LGM-Holocene temperature changes were negligible in the habitat depth range of *Np*1-2 and had no significant effect on the isotopic composition of these morphotypes.

In the late LGM sediments of core PS93/031-5 the $\delta^{18}O$ difference between *Np*1-2 and *Np*4-5 is relatively low (average 0.36‰; Fig. 4) and only half of that seen in Holocene samples. In some LGM samples no significant difference is detectable, considering the average analytical error of ±0.08‰ of isotope measurements. Assuming that, in general, the isotopic composition of *Np*4-5 reflects a shallower habitat than that of the encrusted specimens, the vertical gradient of $\delta^{18}O$ of equilibrium calcite ($\delta^{18}O_{ec}$) in the upper water column was apparently lower than today (Fig. 1), indicating lower salinity differences and a weaker stratification. This may result from comparatively small quantities of liquid freshwater export from the Arctic Ocean and Greenland, as indicated by the high $\delta^{18}O$ values of both *Np*1-2 and *Np*4-5. A strong vertical temperature gradient with higher near-surface temperatures than below is rather unlikely, as indicated by the evidence for a closed sea ice cover discussed below. Presumably, there were smaller differences (if compared to today) of temperature and salinity between both habitats which resulted in an isotopical balance. This assumption is supported by a comparison of the oxygen isotope records from both morphotypes (corrected for the global ice volume effect using the data set of Lisiecki and Stern, 2016) when the $\delta^{18}O_{ec}$ values from ~40 m (mean of 35-45 m) and ~80 m (mean of 70-90 m) are subtracted from the $\delta^{18}O$ values of *Np*4-5 and *Np*1-2, respectively (Fig. 6). While such $\Delta\delta^{18}O$ values of *Np*4-5 from the LGM are in the range of middle Holocene values, the $\Delta\delta^{18}O$ values of *Np*1-2 are more negative than middle Holocene counterparts. Although assumptions of $\delta^{18}O_{ec}$ for the pre-Holocene have to be taken with great caution because of many inherent uncertainties, these more negative values from the LGM may be indicative of somewhat lower salinities at ~80 m and thus a weaker stratification than today. In principle, the similarity of $\delta^{18}O$ values could also result

from a strongly reduced vertical migration of *N. pachyderma* during its life cycle. However, the carbon isotope difference between *Np*1-2 and *Np*4-5 is rather large (average 0.61‰) and suggests that the morphotypes did not inhabit the same water depth. Moreover, *Np*1-2 consistently show higher $\delta^{13}C$ values than *Np*4-5. This is opposite to what can be expected when *Np*4-5 had the shallower habitat and the vertical $\delta^{13}C$ profile were solely the result of *in-situ* carbon cycling in the water column (cf. Mackensen and Schmiedl, 2019). Some caution has to be applied to such considerations, though, because vertical variations in carbonate ion concentrations may have affected the $\delta^{13}C$ of DIC in our research area in the LGM. Today, these vertical variations are very low ($[CO_3^{2-}]$ = 110±10 µmol/kg; Pados et al., 2015) in the upper 500 m of the western Fram Strait, in waters which are supersaturated with calcium carbonate (Anderson et al., 2017). The modern variations could explain only shift of 0.2‰ in $\delta^{13}C$ (cf. Spero et al., 1997), but conditions may have been different in the LGM. The similarity of the relatively high $\delta^{18}O$ values of both morphotypes precludes a strong influence of terrestrial freshwater with a low $\delta^{13}C$ signature as an explanation for the low $\delta^{13}C$ values in shallow living *Np*4-5 during LGM times. They may rather be the result of very limited bioproduction under a perennial sea ice cover.

A thickened cover of rigid sea ice has been proposed for the LGM in the Arctic Ocean (Nørgaard-Pedersen et al., 2003; Bradley and England, 2008) and it is conjecturable that also the major export area for sea ice, the western Fram Strait, was heavily ice-covered. To explain the high $\delta^{13}C$ values of *Np*1-2, we suppose that their deeper habitat was influenced by horizontal advection from the east. High LGM $\delta^{13}C$ values of *Np*1-2 of 0-0.2‰ in cores from the central and eastern Fram Strait stem from a time with seasonally open waters and enhanced planktic bioproduction in that area (Nørgaard-Pedersen et al., 2003), caused by advection of relatively warm Atlantic Water (e.g., Hebbeln et al., 1994; Zamelczyk et al., 2014; Falardeau et al., 2018). Most likely, the $\delta^{13}C$ values in foraminifers from cores from the eastern Fram Strait reflect remineralization of ^{12}C-enriched organic matter below the upper waters with photosynthetic activity. A westward branching (and underway cooling) of this Atlantic Water and its subduction below the halocline, in a basically similar pattern as today (Fig. 1), could explain values of ~0‰ in *Np*1-2 and the relatively high vertical difference of $\delta^{13}C$ values in the western Fram Strait at site PS93/031. A decoupling in terms of carbon cycling is also indicated by the almost constant $\delta^{13}C$ values of *Np*1-2 in the late LGM (0.0‰) which are in contrast to values of 0.6±0.15‰ in *Np*4-5.

The evidence for Atlantic Water advection to the NE Greenland margin in the late LGM has implications for the interpretation of the *Np*1-2 $\delta^{18}O$ values. Together with the rather negative $\Delta\delta^{18}O$ values (Fig. 6), these values, which are ~0.4‰ lower than LGM values in cores from the eastern and central Fram Strait (Nørgaard-Pedersen et al., 2003), may reflect a habitat near the lower halocline which was possibly shallower than today. There, encrustation would add calcite with a high Atlantic Water $\delta^{18}O$ signature to formerly low-$\delta^{18}O$ calcite specimens (for modern analogs see Kozdon et al., 2009). Combined, the oxygen and carbon isotope data of *N. pachyderma* morphotypes suggest a severly ice-covered environment for the western Fram Strait during the late LGM, with a weaker vertical salinity gradient in the upper waters than today, very limited bioproduction, and a noticable advection of Atlantic Water from the east.

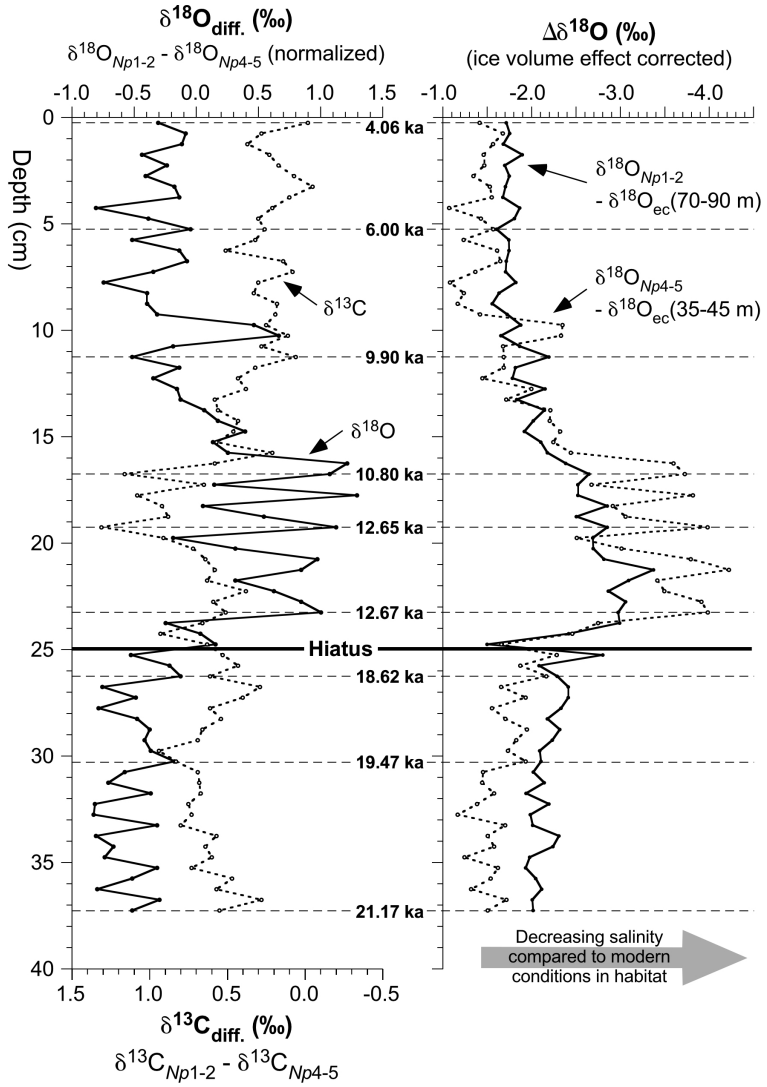

Fig. 6

Left: Differences of oxygen and carbon isotope values between *Np*1-2 and *Np*4-5. Oxygen isotope values are normalized for the $\delta^{18}O$ difference between modern equilibrium calcite calculated values for water depths of 35-45 m (*Np*4-5) and 70-90 m (*Np*1-2) which is ~0.87.

Right: Differences between oxygen isotope records from morphotypes (*Np*1-2 and *Np*4-5, corrected for the global ice volume effect using data of Liesicki and Stern, 2016) and the $\delta^{18}O$ value of modern equilibrium calcite calculated for water depths of 35-45 m (*Np*4-5) and 70-90 m (*Np*1-2). Since temperature variability is minimal in the upper 120 m, lower $\Delta\delta^{18}O$ values indicate lower salinities in the habitat.

5.3. The deglacial freshwater interval

No sediments from the early part of the last glacial-interglacial transition are preserved at site PS93/031. Above the hiatus the $\delta^{18}O$ values of *Np*1-2 and *Np*4-5 are lower by ~1.5‰ and ~3‰, respectively (Fig. 2). Only ~0.5‰ of this change can be attributed to the change of the global ice volume effect between 18.6 and 12.7 ka (cf. Fairbanks, 1989). There is no planktic foraminifer evidence for warmer waters (subpolar planktic foraminifers make up <1% of the

total assemblage in the >100 µm fraction throughout our core). Moreover, records from the eastern Fram Strait and the Nordic Seas show that there was no enhanced heat advection to the Arctic by Atlantic Water before ~10.8 ka (Koç et al., 1993; Sarnthein et al., 2003; Aagaard-Sørensen et al., 2014; Werner et al., 2016). Accordingly, we ascribe the remaining $\delta^{18}O$ difference between 18.6 and 12.7 ka to a major freshwater event at the NE Greenland continental margin which decreased the salinity throughout the upper water column. Due to the hiatus, its onset cannot be determined. The presence of a lag deposit underneath and the uneven boundary to the laminated sediments suggest erosion or selective deposition of mostly coarse IRD due to intense bottom currents. Therefore, the freshwater event may have started some time before 12.7 ka. Other sediment cores from off NE Greenland (Figs. 1, 7) have also recorded a freshwater event at this time. However, their low temporal resolution does not allow a detailed specification of its onset or duration and overall the ages appear somewhat higher than in PS93/031-5 if the IntCal20 data set and R = 550 are applied. The $\delta^{18}O$ record from site PS1230 shows a ~1‰ decrease in one sample (Bauch et al., 2001) which dates to 13.6±0.8 ka (using Calib 8.2 and linear interpolation between ^{14}C-dated samples) or 14.3 ka (using *Bacon*). A ~0.5‰ decrease found in two samples from core PS2887 (Nørgaard-Pedersen et al., 2003) dates to 12.3-13.0 ka. (Calib 8.2) or 12.7-13.2 ka (*Bacon*). In both cores the low $\delta^{18}O$ peaks, measured on *Np*1-2, reach ~2.5‰ and are thus in the same range as in PS93/031-5. Thus, the freshwater event at the NE Greenland continental margin may have been at least a regional phenomenon.

The freshwater provenance cannot be determined from the isotope records presented here. The Greenland ice sheet had advanced beyond the modern coastline on the NE Greenland shelf during the LGM, but it is still debatable whether it reached the shelf break (Funder et al., 2011; Larsen et al., 2018). Morphological features on the shelf sea floor suggest the development of two major ice streams in the Westwind and Norske troughs and the possible development of an ice dome on the shallow bank between the troughs (see Arndt et al., 2017, for a review of available evidence). No datings have been published so far constraining the deglaciation history of the shelf area. However, the disintegration of the ice sheet on the shelf must have released large amounts of freshwater and fine grained sediment. It may be responsible for a strongly reduced salinity just southeast of the mouth of Westwind Trough and the formation of laminated layers at our site on the continental margin. Our data show that the freshwater-affected interval lasted until ~10.2 ka when oxygen isotope values of both *N. pachyderma* morphotypes approached the Holocene level (Fig. 2). The lower calculated sedimentation rates from the layer with faint laminae (deposited ~12.5-10.2 ka) may indicate a two-phase retreat of the ice sheet margin on the NE Greenland shelf towards the modern coastline. A rapid recession early during the event (i.e., before 12.5 ka) with a strong sediment export through Westwind Trough may have been followed by a slower retreat with sediment transport mostly southward through Norske Trough. A lithologic change at ~10.1 in sediment core PS100/270 obtained close to the present-day coastline (Fig. 1a) has been interpreted to reflect the onset of glacimarinemarine sedimentation (Syring et al., 2020a) at this site. Apparently, the last phase of the freshwater event recorded in PS93/031-5 was contemporaneous with the final retreat of the ice sheet to the modern coastline.

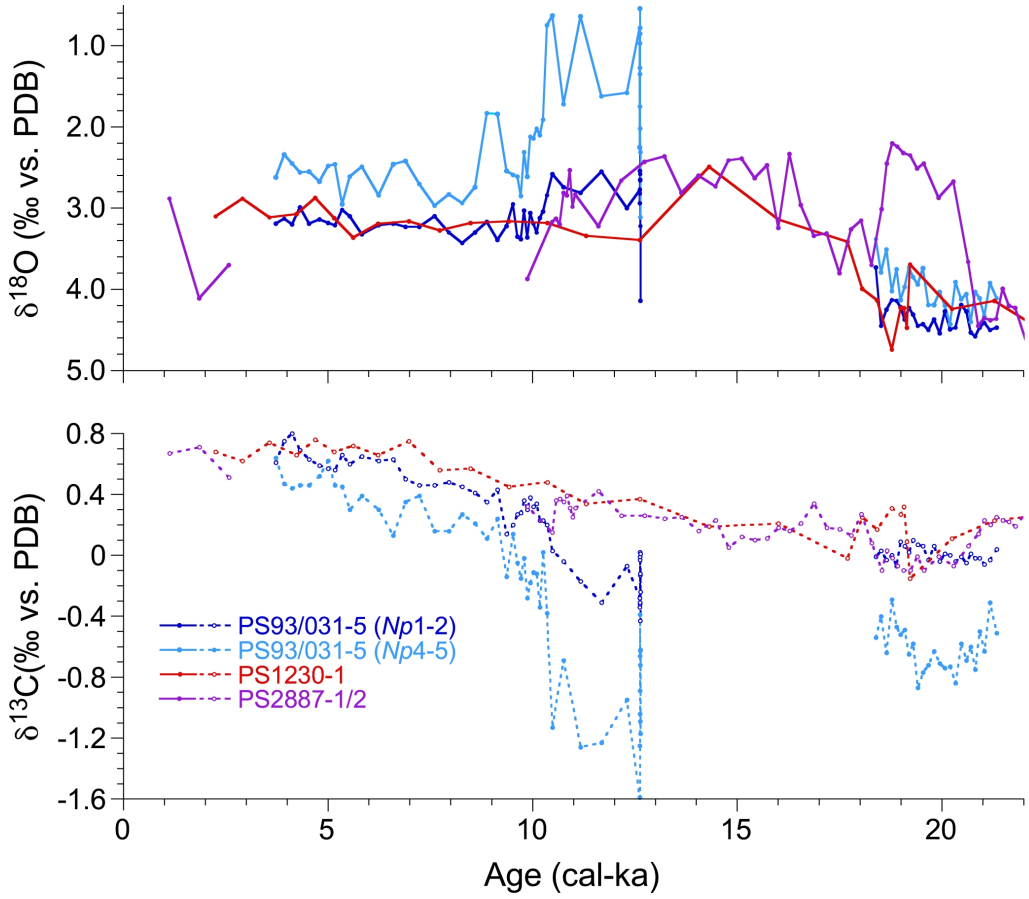

Fig. 7

Stable oxygen and carbon isotope records of *N. pachyderma* from radiocarbon-dated sediment cores from the NE Greenland continental margin (from Nørgaard-Pedersen et al., 2003, and this study). Age models applied were calculated using *Bacon*, the IntCal20 data set, and a reservoir correction of 550 years.

Considering the timing of the early freshwater event, it is remarkable that the oldest dates from the the layer with low $\delta^{18}O$ values are close to the onset of the Younger Dryas event (12.9 ka; Rasmussen et al., 2006). This major cooling was most likely caused by a combination of several factors (Renssen et al., 2015), involving as a major one the freshwater-induced slowdown of the AMOC (Broecker et al., 1985). Recent research suggests that the freshwater outburst occurred through the Mackenzie Valley into the Arctic Ocean (Keigwin et al., 2018). To reach the areas of deepwater convection in the Greenland Sea, the freshwater must have left the Arctic Ocean through Fram Strait. Accordingly, the freshwater spike in $\delta^{18}O$ records from PS93/031-5 and other cores from the western Fram Strait dated 12.5-13.8 ka may also reflect the massive export of meltwater from North American ice sheets which weakened the AMOC and triggered the drastic Younger Dryas cooling in the North Atlantic region. It cannot be excluded, though, that the freshwater outburst in North America and the deglaciation of the NE Greenland shelf were coeval and together contributed to the freshwater event recorded on the continental margin.

The $\delta^{18}O$ differences between *Np*1-2 and *Np*4-5 are 0.7-2.2‰ in the laminated layers from the deglacial freshwater interval recorded in PS93/031-5 (Figs. 2, 4) and can be interpreted to reflect strong and variable salinity differences between the habitat depths of both morphotypes. Apparently, the oxygen isotope composition of *Np*4-5 is a considerably more sensitive recorder than that of *Np*1-2 regarding changes in seawater salinity near the ocean surface caused by the rapid input of freshwater from continental sources (e.g., ice sheet melting/disintegration or ice-dammed lakes). The stronger offset of *Np*4-5 values from the $\delta^{18}O$ of equilibrium calcite (Fig. 6) supports this inference. Applying the modern $\delta^{18}O$/S relationship in the upper ~300 m of the NW Fram Strait (Rabe et al., 2009; Pados et al., 2015), a 2.2‰ difference in $\delta^{18}O$ between the morphotypes is equivalent to a salinity difference of 1.6 practical salinity units (PSU). Since *N. pachyderma* does not live directly at the sea surface, the $\delta^{18}O$ values of *Np*4-5 most likely do not reflect the actual sea surface salinity which must have been significantly lower during the freshwater event than before or after. Today, salinity is ~3 PSU lower at the sea surface than at 40 m water depth (Rabe et al., 2009; Richter et al., 2018). We can use this value as an estimate for the possible vertical salinity difference in the uppermost waters during the freshwater event and arbitrarily assume that $\delta^{18}O$ of *Np*4-5 reflects the salinity at 40 m depth (a value near the shallower end of most depth estimates for the *N.pachyderma* habitat; cf. Greco et al., 2019). When 0.5‰ is accounted for the global ice volume change, the $\delta^{18}O$ change of 3.2‰ in *Np*4-5 between the late LGM and the peak freshwater event would thus imply a salinity decrease of ~4-5 PSU at the sea surface. Such a hypothetic value is slightly above the modern sea surface salinity difference between the Beaufort Sea and our research area (3-4 PSU), as revealed by the World Ocean Atlas 2018 (Boyer et al., 2018; Zweng et al., 2018). We note that it is in the range of the surface salinity perturbation in our research area produced by the model experiment of Condron and Winsor (2012) which simulates the export of freshwater from the Arctic through Fram Strait at the onset of the Younger Dryas event.

The carbon isotope values of the investigated *N.pachyderma* morphotypes from the freshwater interval are exceptionally low (Figs. 2, 4). With one exception, all values are on or below the ~0‰ $\delta^{13}C$ level of *Np*1-2 from the LGM. Like for $\delta^{18}O$, the $\delta^{13}C$ amplitudes in the *Np*4-5 record are 2-3 times larger than those from *Np*1-2. The good correlation (R=0.70) of both $\delta^{13}C$ records suggests that the habitats of both morphotypes were not decoupled in terms of carbon cycling as in the LGM. Instead, we suppose that the low values were caused by the large fraction of continental freshwater in the upper water column. The DIC in modern runoff from high Arctic continental sources like Ellesmere Island, Greenland, and Svalbard is strongly depleted in ^{13}C (Wadham et al., 2004; Long, 2016; St. Pierre et al., 2019). The admixture of freshwater from Greenland, North America and/or other terrestrial sources to the surface waters off NE Greenland must therefore have decreased significantly the $\delta^{13}C$ value of DIC in the near-surface waters during the freshwater event. Since the reduced salinity must have fostered sea ice formation, we assume that bioproduction and the associated preferential ^{12}C uptake were severely limited by a dense sea ice cover so that the uppermost waters remained under the influence of the terrestrial carbon input, depleted in ^{13}C. The low coarse fraction content and the lack of of coarse IRD also point at a perennial ice cover with little

melting. The isotope data do not show any evidence of Atlantic Water at the NE Greenland continental margin in the younger part of the deglaciation documented in core PS93/031-5.

5.4. The Holocene

The increasing amount of coarse fraction and the decreasing isotopic differences between *Np*1-2 and *Np*4-5 between 15 and 12 cm in PS93/031-5 (Fig. 2) indicate that Holocene mean conditions were reached around 9.9 ka, at a time when the Greenland ice sheet had retreated to the present coastline west of site PS93/031 (Syring et al., 2020a). Thereafter, the average $\delta^{18}O$ difference (0.69‰) is less than half of that in the freshwater interval, but almost twice as high as in the late LGM (Fig. 4). It is very similar to the average summer difference in $\delta^{18}Oec$ as calculated by modern oceanographic data from the sector containing our core site (~0.8‰; Fig. 5). This indicates that off NE Greenland the modern water mass structure with a well-expressed halocline was established in the early Holocene. Today, relative changes of calculated $\delta^{18}O_{ec}$ values are minimal (±0.1‰) between 90 and 400 m water depth (Fig. 1), revealing that the temperature increase in and below the halocline is balanced isotopically by an increase of sea water-$\delta^{18}O$ which correlates with the salinity increase. Assuming similar salinity and temperature gradients as today for the halocline in the early and mid-Holocene and applying the modern $\delta^{18}O$/salinity relationship (Rabe et al. 2009; Pados et al, 2015), the average $\delta^{18}O$ difference of 0.69‰ (Fig. 6) between *Np*4-5 (~2.5‰) and *Np*1-2 (~3.2‰) would translate to a salinity difference of only 0.5 PSU. However, we assume that in reality the difference was higher, in particular in the Early Holocene. One reason was probably a significant freshwater runoff from North Greenland glaciers and ice caps which continued to retreat after 10 ka (e.g., Briner et al., 2016; Larsen et al., 2019). Its influence on the isotopic values of *N. pachyderma* can be seen in $\Delta\delta^{18}O$ values between 10 and 9 ka which are somewhat more negative than thereafter (Fig. 6). On the other hand, the Early Holocene in the Fram Strait saw a relatively strong advection of Atlantic Water (e.g., Aagaard-Sørensen et al., 2014; Werner et al., 2016) which also reached the NE Greenland continental margin (Bauch et al., 2001) . High-resolution planktic and benthic $\delta^{18}O$ records from site PS93/025 on the outer NE Greenland shelf (290 m water depth) show very similar values for the 10.6-7.2 ka interval, but Zehnich et al (2020) argue for uniform isotopic values of foraminiferal calcite resulting (i) from low-saline, low-$\delta^{18}O$ waters near the surface and (ii) from unusually warm, high-saline, high-$\delta^{18}O$ Atlantic Water below. A similar situation with an enhanced stratification can be expected for site PS93/031, situated ~130 km further SSE. If the $\delta^{18}O$ of *Np*4-5 reflects shallower conditions and *Np*1-2 integrates its signal over shallow and somewhat deeper waters (cf. Kohfeld et al., 1996), the isotopic difference must be considered a minimum value for the $\delta^{18}O_{ec}$ difference between the *Np*1-2 habitat and the maximum calcification depth, in particular in the Early Holocene when both freshwater runoff and Atlantic Water advection were strongest. While the first depth can be estimated to be around 40 m, the latter was likely in or below the halocline, as suggested by the $\delta^{13}C$ values of Holocene *Np*1-2 in PS93/031-5 discussed further below. If compared to the LGM and the freshwater interval, in the Holocene the differences between $\Delta\delta^{18}O$ values of both morphotypes are rather low (Fig. 6). The differences may still be explained by encrustation of *Np*1-2 in deeper waters. How-

ever, one should be aware that in the early and mid-Holocene the halocline off NE Greenland may have been in a shallower position than today, i.e., under conditions of modern global warming and increased freshwater export from the Arctic (Polyakov et al., 2008; Jahn and Laiho, 2020).

A short period around 8.8 ka with decreased near-surface salinities is recorded by two low $\delta^{18}O$ values of *Np*4-5 only (Fig. 2). Since other records from the area, including the high-resolution Holocene record from site PS93/025 (Zehnich et al., 2020), located ~150 km to the northeast on the outer NE Greenland shelf (Fig. 1a), do not show a coeval peak, it may be related to a regional deglaciation event on Greenland. *A priori* we cannot rule out that Holocene conditions at the NE Greenland margin were punctuated by further short-term freshwater events which cannot be identified in the isotope records due to sediment mixing from bioturbation.

In contrast to the LGM and the freshwater interval, after ~9.9 ka the $\delta^{13}C$ values of *Np*4-5 are only slightly below or even on the same level as those of *Np*1-2 (Figs. 2, 4). Biomarker data from site PS93/025 show that in this period the research area was characterized by a disintegrated or seasonal sea ice cover which allowed a considerable bioproduction (Syring et al., 2020b). Accordingly, we interpret the $\delta^{13}C$ values of *Np*1-2, which are significantly higher than in the LGM and the freshwater interval, as evidence of a relatively strong biological ^{12}C consumption in the upper water column of the Fram Strait. Like for $\delta^{18}O$ of *Np*1-2, the $\delta^{13}C$ values of this morphotype may to a large part reflect the subsurface advection of Atlantic Water from the east, where perennially open waters allow for an even stronger bioproduction than off Greenland and $\delta^{13}C$ values of *Np*1-2 can reach 1‰ (Werner et al., 2013, 2016). The even lower $\delta^{13}C$ values of *Np*4-5 are more difficult to interpret. Pados et al., (2015) tentatively attributed low $\delta^{13}C$ values of planktic foraminifers caught alive in the uppermost waters of the western Fram Strait to the "carbonate ion effect" (Spero et al., 1997). Moreover, the productive zone may have been limited to the uppermost 10-20 m of the water column in the early and mid-Holocene, when sea ice coverage was possibly still denser than today under global warming conditions. Back then, remineralization of organic carbon may have been particularly strong in the habitat of *Np*1-2. Today, the vertical $\delta^{13}C$ record of DIC from 78.8°N, 4°W shows a minimum at 25 m water depth (Pados et al., 2015) and this minimum may have been even more pronounced in the early and mid-Holocene. Overall, the Holocene $\delta^{13}C$ records are more ambiguous than $\delta^{18}O$ data and exemplify the complexity of $\delta^{13}C$ data of DIC in Arctic waters (cf. Bauch et al., 2015).

6. Conclusions

• Stable oxygen and carbon isotope records established on different *Neogloboquadrina pachyderma* morphotypes from sediment cores can significantly improve our ability to investigate the structure of the upper water column in polar waters where other species are largely absent. Although exact calcification depths are not known, the paired records reveal details on the upper ocean stratification that cannot be obtained from single records.

• The isotopic offsets between the investigated morphotypes are different in the three scenarios, which cannot be explained solely by the effect of foraminifer size on the isotopic composition. Changes in water mass parameters and stratification must also be considered.

• The isotope record of thin-shelled specimens is a considerably more sensitive recorder of near-surface salinity changes through time than that of encrusted specimens. During freshwater events, the amplitudes in the records can differ by a factor of 2-4.

• The records from the late LGM reveal a weakly stratified upper water column on the NE Greenland continental margin and only a minor export of freshwater from the Arctic Ocean and Greenland. Bioproduction was strongly reduced, probably by a dense sea-ice cover. There is isotopic evidence for advection of Atlantic Water under the halocline waters.

• Isotope data reveal a deglacial freshwater event off NE Greenland with a sea surface salinity reduction of possibly more than 4 PSU with reference to the LGM and the Holocene. Its onset is not preserved in the record presented here, but it may be coeval with the beginning of the cold Younger Dryas event. The freshwater source cannot be ascertained; it may be connected to the disintegration of the ice sheet on the NE Greenland shelf and/or the export of freshwater from the Arctic Ocean. Most likely. the western Fram Strait was severely ice covered and bioproduction was low.

• The modern water mass structure off NE Greenland with a well-expressed halocline underlain by Atlantic Water was established in the early Holocene at ~9.9 ka. The sea ice coverage was less dense than before and allowed for a considerable planktic bioproduction.

Declaration of interests

The authors declare that they have no known competing financial interests or personal relationships that could have appeared to influence the work reported in this paper.

CRediT author statement

Robert F. Spielhagen: Conceptualization, Methodology, Investigation, Writing - original draft preparation; **Andreas Mackensen:** Investigation, Writing - reviewing and editing.

Data Availability: Data are available at https://doi.pangaea.de/10.1594/PANGAEA.930425.

Acknowledgement

We thank Captain Wunderlich and his crew for the excellent support and cooperation during RV Polarstern cruise PS93.1. We thank the PS93.1 Geoscience Party for support in getting geological shipboard data and sediments, as well as L. Sch€onborn for running and maintai-

ning the mass spectrometers. We are grateful to S. Beil (Univ. Kiel) for help with taking layered photos of N. pachyderma. D. Wangner helped with running the Bacon program. Participation in cruise PS93.1 was supported by the German Federal Ministry for Education and Research (BMBF, grant 03G0833C WTZ RUS System Laptevsee: Transdrift). The study used samples and data provided by AWI (Grant AWI-PS93.1_01). Processing of samples was funded by the Deutsche Forschungsgemeinschaft through the ECHONEG project (grant SP 526/5-1). Constructive comments by the handling editor and two anonymous reviewers greatly helped to improve the earlier version of this article.

References

Aagaard, K., Coachman, L. K.,1968. The East Greenland Current north of Denmark Strait: Part I, Arctic 21, 181–200. https://www.jstor.org/stable/40507537.

Aagaard, K., Swift, J. H., Carmack, E. C. 1985. Thermohaline circulation in the Arctic Mediterranean Seas. J. Geophys. Res. 90, 4833–4846. https://doi.org/10.1029/JC090iC03p04833.

Aagaard Sørensen, S., Husum, K., Werner, K., Spielhagen, R.F., Hald, M., Marchitto, T.M., 2014. A late glacial-early Holocene multiproxy record from the eastern Fram Strait, Polar North Atlantic. Mar. Geol. 355, 15-26. https://doi.org/10.1016/j.margeo.2014.05.009.

Anderson, L.G., Ek, J., Ericson, Y., Humborg, C., Semiletov, I., Sundbom, M., Ulfsbo, A., 2017. Export of calcium carbonate corrosive waters from the East Siberian Sea. Biogeosci. 14, 1811–1823. https://doi.org/10.5194/bg-14-1811-2017.

Arndt, J.E., Jokat, W., Dorschel, B., 2017. The last glaciation and deglaciation of the Northeast Greenland continental shelf revealed by hydro-acoustic data. Quat. Sci. Rev. 160, 45–56. https://doi.org/10.1016/j.quascirev.2017.01.018.

Bauch, D., Carstens, J., Wefer G., 1997. Oxygen isotope composition of living *Neogloboquadrina pachyderma* (sin) in the Arctic Ocean. Earth Planet. Sci. Lett. 146 (1–2), 47–58. https://doi.org/10.1016/S0012-821X(96)00211-7.

Bauch, D., Polyak, L., Ortiz, J.D., 2015. A baseline for the vertical distribution of the stable carbon isotopes of dissolved inorganic carbon ($\delta^{13}C_{DIC}$) in the Arctic Ocean. Arktos 1, 15. https://doi.org/10.1007/s41063-015-0001-0.

Bauch, D., Schlosser, P., Fairbanks, R.G., 1995. Freshwater balance and the sources of deep and bottom waters in the Arctic Ocean inferred from the distribution of H218O. Progr. Oceanogr. 35 (1), 53-80. https://doi.org/10.1016/0079-6611(95)00005-2.

Bauch, H.A., Erlenkeuser, H., Spielhagen, R.F., Struck, U., Matthiessen, J., Thiede, J., Heinemeier, J., 2001. A multiproxy reconstruction of the evolution of deep and surface waters in the subarctic Nordic seas over the last 30,000 yr. Quat. Sci. Rev. 20, 659-678. https://doi.org/10.1016/S0277-3791(00)00098-6.

Bemis, B.E., Spero, H.J., Bijma, J., Lea, D.W., 1998. Reevaluation of the oxygen isotopic composition of planktonic foraminifera: Experimental results and revised paleotemperature equations, Paleoceanography, 13, 150–160, 1998. https://doi.org/10.1029/98PA00070.

Berberich, D., 1996. Die planktische Foraminifere *Neogloboquadrina pachyderma* (Ehrenberg) im Weddellmeer, Antarktis. Ber. Polarforschung 195, 193 p. https://epic.awi.de/id/eprint/26373/1/BerPolarforsch1996195.pdf.

Blaauw, M., Christen, J.A., 2011. Flexible paleoclimate age-depth models using an autoregressive gamma process. Bayesian Analysis 6 (3), 457-474. https://doi.org/10.1214/11-BA618.

Boyer, T.P., Garcia, H.E., Locarnini, R.A., Zweng, M.M., Mishonov, A.V., Reagan, J.R., Weathers, K.A., Baranova, O.K., Seidov, D., Smolyar, I.V., 2018. World Ocean Atlas 2018, NOAA National Centers for Environmental Information. https://accession.nodc.noaa.gov/NCEI-WOA18, accessed 2021-6-3.

Bradley, R.S., England, J.H., 2008. The Younger Dryas and the sea of ancient ice. Quat. Res. 70, 1–10. doi:10.1016/j.yqres.2008.03.002.

Briner, J.P., McKay, N.P., Axford, Y., Bennike, O., Bradley, R.S., de Vernal, A., Fisher, D., Francus, P., Frechette, B., Gajewski, K., Jennings, A., Kaufman, D.S., Miller, G., Rouston, C., Wagner, B., 2016. Holocene climate change in Arctic Canada and Greenland. Quat. Sci. Rev. 147, 340–364. https://doi.org/10.1016/j.quascirev.2016.02.010.

Broecker, W.S., Peteet, D.M., Rind, D., 1985. Does the ocean-atmosphere system have more than one stable mode of operation?. Nature 315, 21-26. https://doi.org/10.1038/315021a0.

Carstens, J., Hebbeln, D., Wefer, G., 1997. Distribution of planktic foraminifera at the ice margin in the Arctic (Fram Strait). Mar. Micropal. 29, 257-269. https://doi.org/10.1016/S0377-8398(96)00014-X.

Condron, A., Winsor, P., 2012. Meltwater routing and the Younger Dryas. Proc. Natl. Acad. Sci. 109(49), 19928–19933. https://doi.org/10.1073/pnas.1207381109.

Coulthard, R.D., Furze, M.F.A., Pienkowski,A.J., Nixon, F.C., England, J.E., 2010. New marine ΔR values for Arctic Canada. Quat. Geochronol. 5 (4), 419-434. https://doi.org/10.1016/j.quageo.2010.03.002.

De Steur, L., Hansen, E., Mauritzen, C., Beszczynska-Möller, A., Fahrbach, E., 2014. Impact of recirculation on the East Greenland Current in Fram Strait: Results from moored current meter measurements between 1997 and 2009. Deep-Sea Res. 92, 26–40. https://doi.org/10.1016/j.dsr.2014.05.018.

Dickson, R., Rudels, B., Dye, S., Karcher, M., Meincke, J., Yashayaev, I., 2007. Current estimates of freshwater flux through the Arctic and Subarctic seas. Prog. Oceanogr. 73, 210–230. https://doi.org/10.1016/j.pocean.2006.12.003.

El Bani Altuna, N., Pieńkowski, A.J., Eynaud, F., Thiessen, R., 2018. The morphotypes of *Neogloboquadrina pachyderma*: Isotopic signature and distribution patterns in the Canadi-

an Arctic Archipelago and adjacent regions. Mar. Micropal. 142, 13-24. https://doi.org/10.1016/j.marmicro.2018.05.004

Epstein, S., Buchsbaum, R., Lowenstamm, H.A., Urey, H.C., 1953. Revised carbonate water isotopic temperature scale. Geol. Soc. Amer. Bull. 64, 1315–1325. https://doi.org/10.1130/0016-7606(1953)64[1315:RCITS]2.0.CO;2.

Eynaud, F., 2011. Planktonic foraminifera in the Arctic: potentials and issues regarding modern and Quaternary assemblages. In: IOP Conf. Ser.: Earth Envir. Sci. 14, 012005. http://dx.doi.org/10.1088/1755-1315/14/1/012005.

Eynaud, F., Cronin, T.M., Smith, S., Zaragosi, S., Mavel, J., Mary, Y., Mas, V., Pujol, C., 2009. Morphological variability of the planktonic foraminifer *Neogloboquadrina pachyderma* from ACEX cores: Implications for Late Pleistocene circulation in the Arctic Ocean. Micropal. 55 (2-3), 101-116. http://www.jstor.org/stable/40607109.

Fairbanks, R.G., 1989. A 17 000-year glacio-eustatic sea-level record: Influence of glacial melting rates on the Younger Dryas event and deep ocean circulation. Nature 342, 637–642. https://doi.org/10.1038/342637a0.

Falardeau, J., de Vernal, A., Spielhagen, R.F., 2018. Paleoceanography of northeastern Fram Strait since the last glacial maximum: Palynological evidence of large amplitude changes. Quat. Sci. Rev. 195, 133-152. doi.org/10.1016/j.quascirev.2018.06.030.

Fogel, M.L., Cifuentes, L.A., 1993. Isotope fractionation during primary production. In: Organic Geochemistry. Topics in Geobiology 11. Springer, Boston, MA. https://doi.org/10.1007/978-1-4615-2890-6_3.

Funder, S., Kjeldsen, K.K., Kjær, K.H., O Cofaigh, C., 2011. The Greenland Ice Sheet during the past 300,000 years: a review. In: Ehlers, J., Gibbard, P., Hughes, P. (eds.), Quaternary Glaciations - Extent and Chronology, Part IV: a Closer Look, pp. 699-713. https://doi.org/10.1016/B978-0-444-53447-7.00050-7.

Greco, M., Jonkers, L., Kretschmer, K., Bijma, J., Kucera, M., 2019. Depth habitat of the planktonic foraminifera *Neogloboquadrina pachyderma* in the northern high latitudes explained by sea-ice and chlorophyll concentrations. Biogeosci., 16, 3425-3437. https://doi.org/10.5194/bg-16-3425-2019.

Healy-Williams, N., 1992. Stable isotope differences among morphotypes of *Neogloboquadrina pachyderma* (Ehrenberg): implications for high-latitude palaeoceanographic studies. Terra Nova, 4,693-700, 1992. https://doi.org/10.1111/j.1365-3121.1992.tb00619.x.

Heaton, T.J., Köhler, P., Butzin, M., Bard, E., Reimer, R.W., Austin, W.E.N., Bronk Ramsey, C., Hughen, K.A., Kromer, B., Reimer, P.J., Adkins, J., Burke, A., Cook, M.S., Olsen, J., Skinner, L.C., 2020. MARINE20 - the marine radiocarbon age calibration curve (0-55,000 cal BP). Radiocarbon 62. https://doi.org/10.1017/RDC.2020.68.

Hebbeln, D., Dokken, T., Andersen, E.S., Hald, M., Elverhøi, A., 1994. Moisture supply for northern ice-sheet growth during the Last Glacial Maximum. Nature 370, 357–360. https://doi.org/10.1038/370357a0.

Hillaire-Marcel, C., De Vernal, A., Polyak, L., Darby, D., 2004. Size-dependent isotopic composition of planktic foraminifers from Chukchi Sea vs. NW Atlantic sediments – Implications for the Holocene paleoceanography of the western Arctic. Quat. Sci. Rev. 23, 245–260. https://doi.org/10.1016/j.quascirev.2003.08.006, 2004.

Håvik, L., Pickart, R., Våge, K., Torres, D., Thurnherr, A., Beszczynska-Möller, A., Walczowski, W., and von Appen, W.-J., 2017. Evolution of the East Greenland Current from Fram Strait to Denmark Strait: Synoptic measurements from summer 2012, J. Geophys. Res. Oceans 122, 1974–1994. https://doi.org/10.1002/2016JC012228.

Jackson, L., Wood, R., 2018. Timescales of AMOC decline in response to freshwater forcing. Clim. Dyn. 51, 1333-1350. https://doi.org/10.1007/s00382-017-3957-6

Jahn, A., Laiho, R., 2020. Forced changes in the Arctic freshwater budget emerge in the early 21st century. Geophys. Res. Lett., 47, e2020GL088854. https://doi.org/10.1029/2020GL088854.

Jensen, S., 1998. Planktische Foraminiferen im Europäischen Nordmeer: Verbreitung und Vertikalfluss sowie ihre Verbreitung während der letzten 15000 Jahre. Ber. Sonderforschungsbereich 313, 75, 105 pp.

Jonkers, L., van Heuven, S., Zahn, R., Peeters, F.J.C., 2013. Seasonal patterns of shell flux, $\delta^{18}O$ and $\delta^{13}C$ of small and large *N. pachyderma* (s) and *G. bulloides* in the subpolar North Atlantic. Paleoceanography 28, 164–174. https://doi:10.1002/palo.20018.

Kanzow, T., von Appen, W.-J., Schaffer, J., Köhn, E., Tsubouchi, T., Wilson, N., Wisotzki, A., 2017. Physical oceanography measured with CTD/Large volume Watersampler-system during POLARSTERN cruise PS100 (ARK-XXX/2). Alfred Wegener Institute, Helmholtz Centre for Polar and Marine Research, Bremerhaven, PANGAEA, https://doi.org/10.1594/PANGAEA.871025.

Kaminski, M. A. & Niessen, F. (and the PS87 Shipboard Geoscience Party), 2015. Modern agglutinated Foraminifera from the Hovgård Ridge, Fram Strait, west of Spitsbergen: evidence for a deep bottom current. Ann. Soc. Geol. Pol., 85, 309–320. https://doi.org/10.14241/asgp.2015.006.

Keigwin, L.D., Klotsko, S., Zhao, N., Reilly, B., Giosan, L., Driscoll, N.W., 2018. Deglacial floods in the Beaufort Sea preceded Younger Dryas cooling. Nat. Geosci. 11, 599–604 https://doi.org/10.1038/s41561-018-0169-6.

Koç, N., Jansen, E., Haflidason, H., 1993. Paleoceanographic reconstructions of surface ocean conditions in the Greenland, Iceland and Norwegian seas through the last 14 ka based on diatoms. Quat. Sci. Rev. 12, 115-140. https://doi.org/10.1016/0277-3791(93)90012-B.

Kohfeld, K.E., Fairbanks, R.G., Smith, S.L., Walsh, I.D., 1996. *Neogloboquadrina pachyderma* (sinistral coiling) as paleoceanographic tracers in polar oceans: Evidence from Northeast Water Polynya plankton tows sediment traps and surface sediments Paleoceanography 11 (6), 679-699. https://doi.org/10.1029/96pa02617, 1996.

Kozdon, R., Ushikubo, T., Kita, N.T., Spicuzza, M., Valley, J.W., 2009. Intratest oxygen isotope variability in the planktonic foraminifer *N. pachyderma*: Real vs. apparent vital effects by ion microprobe. Chem. Geol. 258 (3–4), 327–337. https://doi.org/10.1016/j.chemgeo.2008.10.032.

Kroopnick, P., 1974. The dissolved O_2-CO_2-^{13}C system in the eastern equatorial Pacific. Deep-Sea Res. 21, 211–227. https://doi.org/10.1016/0011-7471(74)90059-X.

Larsen, N.K., Levy, L.B., Carlson, A. E., Buizert, C., Olsen, J., Strunk, A., Bjørk, A.A., Skov, D.S., 2018. Instability of the Northeast Greenland Ice Stream over the last 45,000 years. Nat. Commun. 9, 1872. https://doi.org/10.1038/s41467-018-04312-7.

Larsen, N.K., Levy, L.B., Strunk, A., Søndergaard, A.S., Olsen, J.,Lauridsen, T.L. 2019. Local ice caps in Finderup Land, North Greenland, survived the Holocene Thermal Maximum. Boreas 48, 551–562. https://doi.org/10.1111/bor.12384.

Lisiecki, L.E., Stern, J.V., 2016. Regional and global benthic $\delta^{18}O$ stacks for the last glacial cycle. Paleoceanogr. Paleoclim. 31, 2016PA003 002, https://doi.org/10.1002/2016PA003002.

Locarnini, R.A., Mishonov, A.V., Baranova, O.K., Boyer, T.P., Zweng, M.M., Garcia, H.E., Reagan, J.R., Seidov, D., Weathers, K., Paver, C.R., Smolyar, I., 2018. World Ocean Atlas 2018, v. 1: Temperature. A. Mishonov, Technical Ed., NOAA Atlas NESDIS 81, 52 pp.

Long, H.E., 2016. New insight into the drivers, magnitude and sources of fluvial CO_2 efflux in temperate and arctic catchments. PhD thesis, Univ. Glasgow, Dec. 2016, 212 pp. http://theses.gla.ac.uk/7963/.

Mackensen, A., Schmiedl, G., 2019. Stable carbon isotopes in paleoceanography: atmosphere, oceans, and sediments. Earth Sci. Rev. 197, 102893. https://doi.org/10.1016/j.earscirev.2019.102893.

Manabe, S., Stouffer, R.J., 1995. Simulation of abrupt climate-change induced by fresh-water input to the North-Atlantic Ocean. Nature 378, 165-167. https://doi.org/10.1038/378165a0.

Mangerud, J., Bondevik, S., Gulliksen, S., Hufthammer, A.K., Høisæter, T., 2006. Marine ^{14}C reservoir ages for 19th century whales and molluscs from the North Atlantic. Quat. Sci. Rev. 25, 3228-3245. https://doi:10.1016/j.quascirev.2006.03.010.

Manley, T., 1995. Branching of Atlantic Water within the Greenland-Spitsbergen Passage: An estimate of recirculation. J. Geophys. Res. 100, 20627–20634. https://doi.org/10.1029/95JC01251.

Mix, A.C., Bard, E., Schneider, R., 2001. Environmental processes of the ice age: land, oceans, glaciers (EPILOG). Quat. Sci. Rev. 20, 627-657. https://doi.org/10.1016/S0277-3791(00)00145-1.

Nyland, B.F., Jansen, E., Elderfield, H., Andersson, 2006. *Neogloboquadrina pachyderma* (dex. and sin.) Mg/Ca and $\delta^{18}O$ records from the Norwegian Sea. Geochem. Geophys. Geosyst., 7, Q10P17, doi:10.1029/2005GC001055.

Nørgaard-Pedersen, N., Mikkelsen, N., Kristoffersen, Y., 2008. Late glacial and Holocene marine records from the Independence Fjord and Wandel Sea regions, north Greenland. Polar Res. 27, 209–221. https://doi:10.1111/j.1751-8369.2008.00065.x

Nørgaard-Pedersen, N., Spielhagen, R.F., Erlenkeuser, H., Grootes, P.M., Heinemeier, J., Knies, J., 2003. Arctic Ocean during the Last Glacial Maximum: Atlantic and polar domains of surface water mass distribution and ice cover. Paleoceanography 18 (3), 1063. https://doi.org/10.1029/2002PA000781.

O'Neil, J.R., Clayton, R.N., Mayeda, T.K., 1969. Oxygen isotope fractionation in divalent metal carbonates. J. Chem. Phys. 51, 5547–5558. https://doi.org/10.1063/1.1671982.

Pados, T., Spielhagen, R.F., 2014. Species distribution and depth habitat of recent planktic foraminifera in Fram Strait, Arctic Ocean. Polar Res. 33 (1), 22483. https://doi.org/10.3402/polar.v33.22483.

Pados T., Spielhagen R.F., Bauch D., Meyer H., Segl M., 2015. Oxygen and carbon isotope composition of modern planktic foraminifera and near-surface waters in the Fram Strait (Arctic Ocean) – A case-study. Biogeosci. 12, 1733–1752. https://doi.org/10.5194/bg-12-1733-2015.

Polyakov, I.V., Alexeev, V.A., Belchansky, G.I., Dmitrenko, I.A., Ivanov, V.V., Kirillov, S.A., Korablev, A.A., Steele, M., Timokhov, L.A., Yashayaev, I., 2008. Arctic Ocean freshwater changes over the past 100 years and their causes. J. Clim. 21, 364– 384. https://doi.org/10.1175/2007JCLI1748.1

Rabe, B., Schauer, U., Mackensen, A., Karcher, M., Hansen, E.,Beszczynska-Möller, A., 2009. Freshwater components and transports in the Fram Strait: - recent observations and changes since the late 1990s. Ocean Sci., 5, 219-233. https://doi.org/10.5194/os-5-219-2009.

Rahmstorf, S., Box, J.E., Feulner, G., Mann, M.E., Robinson, A., Rutherford, S., Schaffernicht, E.J., 2015. Exceptional twentieth century slowdown in Atlantic Ocean overturning circulation. Nat. Clim. Change 5, 475–480. https://doi.org/10.1038/nclimate2554.

Rasmussen, S.O., Andersen, K.K., Svensson, A.M., Steffensen, J.P.,Vinther, B.M., Clausen, H.B., Siggaard-Andersen, M.-L., Johnsen, S.J., Larsen, L.B., Dahl-Jensen, D., Bigler, M., Röthlisberger, R., Fischer, H., Goto-Azuma, K., Hansson, M.E., Ruth, U., 2006. A new Greenland ice core chronology for the last glacial termination. J. Geophys. Res. 111, D06102. https://doi.org/10.1029/2005JD006079

Renssen, H., Mairesse, A., Goosse, H., Mathiot, P., Heiri, O., Roche, D.M., Nisancioglu, K.H., Valdes, P.J., 2015. Multiple causes of the Younger Dryas cold period. Nat. Geosci. 8, 946–950. https://doi.org/10.1038/ngeo2557.

Richter, M.E., von Appen, W.-J., Wekerle, C., 2018. Does the East Greenland Current exist in the northern Fram Strait? Ocean Sci. 14, 1147–1165. https://doi.org/10.5194/os-14-1147-2018.

Rudels, B., Korhonen, M., Budéus, G., Beszczynska-Möller, A., Schauer, U., Nummelin, A., Quadfasel, D., and Valdimarsson, H. 2012. The EastGreenland Current and its impacts on the Nordic Seas: observed trends in the past decade. ICES J. Mar. Sci. 69(5), 841–851. https://doi.org/10.1093/icesjms/fss079.

Sarnthein, M., Jansen, E., Weinelt, M.S., Arnold, M., Duplessy, J.C., Erlenkeuser, H., Flatøy, A., Johannessen, G., Johannessen, T., Jung, S.J.A., Koç, N., Labeyrie, L.D., Maslin, M., Pflaumann, U., Schulz, H., 1995. Variations in Atlantic surface ocean paleoceanography, 50-80°N: a time-slice record of the last 30,000 years. Paleoceanography 10, 1063-1094. https://doi.org/10.1029/95PA01453.

Sarnthein, M., van Krefeld, S., Erlenkeuser, H., Grootes, P.M., Kucera, M., Pflaumann, U., Schulz, M., 2003. Centennial-to-millennial-scale periodicities of Holocene climate and sediment injections off the western Barents shelf, 75°N. Boreas 32, 447-461. https://doi.org/10.1111/j.1502-3885.2003.tb01227.x.

Schiebel, R., Spielhagen, R.F., Garnier, J., Hageman, J., Howa, H., Jentzen, A., Martínez-Garcia, A., Meilland, J., Michel, E., Repschläger, J., Salter, I., Yamasaki, M., Haug, G., 2017. Modern planktic foraminifers in the high-latitude ocean. Mar. Micropal. 136, 1-13. http://dx.doi.org/10.1016/j.marmicro.2017.08.004.

Schlitzer, R., 2020. Ocean Data View, https://odv.awi.de.

Schmitt, J., Schneider, R., Elsig, J., Leuenberger, D., Lourantou, A., Chappellaz, J., Kohler, P., Joos, F., Stocker, T.F., Leuenberger, M., Fischer, H., 2012. Carbon isotope constraints on the deglacial CO_2 rise from ice cores. Science 336, 711-714. https://doi.org/10.1126/science.1217161.

Simstich, J., Sarnthein, M., Erlenkeuser, H., 2003. Paired δ18O signals of *Neogloboquadrina pachyderma* (s) and *Turborotalita quinqueloba* show thermal stratification structure in Nordic Seas. Mar. Micropaleontol. 48 (1-2), 107-125. https://doi.org/10.1016/S0377-8398(02)00165-2.

Spero, H.J., Bijma, J., Bemis, B., Lea, D., 1997. Effects of sea water carbonate chemistry on planktonic foraminifera carbon and oxygen isotope values. Nature, 390, 497-500. https://doi.org/10.1038/37333.

Spielhagen R.F., Bauch H.A., 2015. The role of Arctic Ocean freshwater during the past 200 ky. Arktos. http://dx.doi.org/10.1007/s41063-015-0013-9.

Spielhagen, R. F., Baumann, K.-H., Erlenkeuser, H., Nowaczyk, N. R., Nørgaard-Pedersen, N., Vogt, C., and Weiel, D., 2004. Arctic Ocean deep-sea record of Northern Eurasian ice sheet history. Quat. Sci. Rev. 23 (11-13), 1455-1483. https://doi.org/10.1016/j.quascirev.2003.12.015.

Stein, R., 2015. Documentation of sediment core PS93/031-5. Alfred Wegener Institute - Polarstern core repository, PANGAEA, https://doi.org/10.1594/PANGAEA.855080.

Stein, R., 2016. The Expedition PS93.1 of the Research Vessel POLARSTERN to the Greenland Sea and the Fram Strait in 2015. Rep. Polar Mar. Res. 695 , 151 p. http://doi.org/10.2312/BzPM_0695_2016.

St. Pierre, K.A., St. Louis, V.L., Schiff, S.L., Lehnherr, I., Dainard, P.G., Gardner, A.S., Aukes, P.J.K., Sharp, M.J., 2019. Proglacial freshwaters are significant and previously unrecognized sinks of atmospheric CO_2. Proc. Natl. Acad. Sci. 116 (36), 17690–17695. https://doi.org/10.1073/pnas.1904241116.

Stuiver, M., Reimer, P.J., Reimer, R.W., 2021. CALIB 8.2 [WWW program] at http://calib.org, accessed 2021-1-27.

Syring, N., Lloyd, J.M., Stein, R., Fahl, K., Roberts, D.H., Callard, L., O'Cofaigh, C., 2020a. Holocene interactions between glacier retreat, sea-ice formation and Atlantic Water advection at the inner Northeast Greenland continental shelf. Paleoceanogr. Paleoclim. 35, e2020PA004019.https://doi.org/10.1029/2020PA004019.

Syring, N., Stein, R., Fahl, K., Vahlenkamp, M., Zehnich, M., Spielhagen, R.F., Niessen, F., 2020b. Holocene changes in sea-ice cover and polynya formation along the eastern North Greenland shelf: New insights from biomarker records. Quat. Sci. Rev. 231, 106173. https://doi.org/10.1016/j.quascirev.2020.106173.

Tauber, H., Funder S., 1975. ^{14}C content of recent molluscs from Scoresby Sund, central East Greenland. Grønlands Geol. Unders. Rapp. 75, 95–99.

Van Nieuwenhove, N., Limoges. A., Nørgaard-Pedersen, N., Seidenkrantz, M.-S., Ribeiro, S., 2020. Episodic Atlantic Water inflow into the Independence Fjord system (Eastern North Greenland) during the Holocene and last glacial period. Front. Earth Sci. 8, 565670. https://doi: 10.3389/feart.2020.565670.

Wadham, J.L., Bottrell, S., Tranter, M., Raiswell, R., 2004. Stable isotope evidence for microbial sulphate reduction at the bed of a polythermal high Arctic glacier. Earth Planet. Sci. Lett. 219, 341–355. https://doi.org/10.1016/S0012-821X(03)00683-6.

Werner, K., Müller, J., Husum, K., Spielhagen, R.F., Kandiano, E.S., Polyak, L., 2016. Holocene sea subsurface and surface water masses in the Fram Strait – Comparisons of temperature and sea-ice reconstructions. Quat. Sci. Rev. 147, 194-209. https://doi.org/10.1016/j.quascirev.2015.09.007.

Werner, K., Spielhagen, R.F., Hass, H.C., Bauch, D., Kandiano, E., Struve, T., 2013. Atlantic Water advection versus sea ice advances in the eastern Fram Strait during the last 9 ka – multiproxy evidence for a two-phase Holocene. Paleoceanography, 28, 283-295. http://dx.doi.org/10.1002/palo.20028.

Xiao, W., Wang, R., Polyak, L., Astakhov, A., Cheng, X., 2014. Stable oxygen and carbon isotopes in planktonic foraminifera Neogloboquadrina pachyderma in the Arctic Ocean: an overview of published and new surface-sediment data. Mar. Geol. 352, 397-408. http://dx.doi.org/10.1016/j.margeo.2014.03.024.

Zamelczyk, K., Rasmussen, T., Husum, K., Godtliebsen, F., Hald, M., 2014. Surface water conditions and calcium carbonate preservation in the Fram Strait during marine isotope stage 2, 28.8-15.4 kyr. Paleoceanography 29, 1-12. https://doi.org/10.1002/2012PA002448.

Zehnich, M., Spielhagen, R.F., Bauch, H.A., Forwick, M., Hass, H.C., Palme, T., Stein, R., Syring, N., 2020. Environmental variability off NE Greenland (western Fram Strait) during the past 10,600 years. The Holocene. https://doi.org/10.1177/0959683620950393.

Zweng, M.M., Reagan, J.R., Seidov, D., Boyer, T.P., Locarnini, R.A., Garcia, H.E., Mishonov, A.V., Baranova, O.K., Weathers, K., Paver, C.R., Smolyar, I., 2018. World Ocean Atlas 2018, v. 2: Salinity, A. Mishonov, Technical Ed., NOAA Atlas NESDIS 82, 50 pp.